



저작자표시-비영리-변경금지 2.0 대한민국

이용자는 아래의 조건을 따르는 경우에 한하여 자유롭게

- 이 저작물을 복제, 배포, 전송, 전시, 공연 및 방송할 수 있습니다.

다음과 같은 조건을 따라야 합니다:



저작자표시. 귀하는 원저작자를 표시하여야 합니다.



비영리. 귀하는 이 저작물을 영리 목적으로 이용할 수 없습니다.



변경금지. 귀하는 이 저작물을 개작, 변형 또는 가공할 수 없습니다.

- 귀하는, 이 저작물의 재이용이나 배포의 경우, 이 저작물에 적용된 이용허락조건을 명확하게 나타내어야 합니다.
- 저작권자로부터 별도의 허가를 받으면 이러한 조건들은 적용되지 않습니다.

저작권법에 따른 이용자의 권리는 위의 내용에 의하여 영향을 받지 않습니다.

이것은 [이용허락규약\(Legal Code\)](#)을 이해하기 쉽게 요약한 것입니다.

[Disclaimer](#)

A THESIS FOR THE DEGREE OF MASTER OF SCIENCE

**Curing Behavior and Characterization of Dual Curable
Adhesives Based on Azo-initiator with High Reactivity
for Touch Screen Panel in Display**

디스플레이 터치 스크린 패널 공정을 위한
고반응성 아조계 열개시제 기반의
이중경화형 접착제의 경화거동 및 물성 평가

by Jong-Gyu Lee

PROGRAM IN ENVIRONMENTAL MATERIALS SCIENCE

GRADUATE SCHOOL

SEOUL NATIONAL UNIVERSITY

AUGUST, 2015

A THESIS FOR THE DEGREE OF MASTER OF SCIENCE

**Curing Behavior and Characterization of Dual Curable
Adhesives Based on Azo-initiator with High Reactivity
for Touch Screen Panel in Display**

디스플레이 터치 스크린 패널 공정을 위한
고반응성 아조계 열개시제 기반의
이중경화형 접착제의 경화거동 및 물성 평가

by Jong-Gyu Lee

Advisor: Hyun-Joong Kim

PROGRAM IN ENVIRONMENTAL MATERIALS SCIENCE

GRADUATE SCHOOL

SEOUL NATIONAL UNIVERSITY

AUGUST, 2015

**Curing Behavior and Characterization of Dual Curable
Adhesives Based on Azo-initiator with High Reactivity
for Touch Screen Panel in Display**

디스플레이 터치 스크린 패널 공정을 위한
고반응성 아조계 열개시제 기반의
이중경화형 접착제의 경화거동 및 물성 평가

지도교수: 김 현 중

이 논문을 농학석사학위논문으로 제출함

2015년 5월

서울대학교 대학원
산림과학부 환경재료과학 전공
이 중 규

이중규의 석사학위논문을 인준함

2015년 7월

위 원 장 최 인 규 (인)

부위원장 김 현 중 (인)

위 원 윤 혜 정 (인)

Abstract

Curing Behavior and Characterization of Dual Curable Adhesives Based on Azo-initiator with High Reactivity for Touch Screen Panel in Display

Jong-Gyu Lee

Program in Environmental Materials Science

Graduate School

Seoul National University

Dual curing was introduced to improve the conversion of optically clear resin (OCR) on shadowed area of display bonding process. The application of UV curing is increased due to the distinct advantages such as fast curing rate, low ambient temperature and solvent-free process. However, UV curing can cause curing problem in shadowed area or curved area, which inhibits UV light penetration. Up till now, only UV curing process with side UV irradiation was applied in touch screen panel bonding process. Curing problem was an issue especially in display bonding process because UV light could not penetrate black matrix (BM) area of the window. Therefore, dual curing system was researched to improve the conversion at shadowed area.

In this study, 2,2'-azobis(4-methoxy-2,4-dimethyl valeronitrile), the thermal radical initiator with 30°C of 10 hour half-life decomposition temperature, was used for granting ability of thermal curing in the low curing temperature. Compared to other dual curing methods, the radical dual curing system did not remain the unreacted functional group after curing. Also, changing thermal initiator easily controlled the reaction temperature. Acrylic prepolymer was synthesized by UV bulk polymerization using 2-ethylhexyl acrylate (2-EHA), isobornyl acrylate (IBA) and N-vinyl caprolactam (VC)

with 1phr of hydroxydimethyl acetophenone as photo radical initiator. Dual curable adhesives were prepared by blending prepolymer with poly(ethyleneglycol (200) dimethacrylate) and thermal radical initiator. The thermal radical initiator, 2,2'-azobis(4-methoxy-2,4-dimethyl valeronitrile), was added under 0.1phr of the resin without problems such as stability, yellowing and bubbling issue. Also, dual curable adhesives was cured with various UV doses (0, 400, 800 and 1600 mJ/cm²) because progress of UV light was hindered by FPCB or BM area of the display in the bonding process.

The curing behavior of dual curable adhesives was investigated by using Fourier transform infrared spectroscopy-attenuated total reflectance (FTIR-ATR), photo-differential scanning calorimetry (photo-DSC) and UV-advanced rheometric expansion system (UV-ARES). Thermal curing efficiency was increased as the concentration of thermal initiator increased. Also, 0.1phr of thermal initiator contents provided enough conversion of the adhesives. Thermal curing efficiency was decreased as the UV dose increases due to the decreasing mobility of the polymer. However, thermal initiation was accelerated in low UV dose condition. Gel fraction results showed that network structure was formed additionally by thermal curing, but none of the network structure of the dual cured adhesive was formed over 800 mJ/cm² UV dose. Conversion and degree of crosslinking could be obtained by accelerating thermal curing efficiency. However, adhesive with 800 mJ/cm² UV dose which the thermal curing was suppressed had lower crosslinking density and conversion than adhesive with 400 mJ/cm² UV dose. In addition, thermal resistance and glass transition temperature was increased by thermal initiator reaction. It is assumed that the formation of a temporary crosslinking structure was produced through the reaction of residual monomer and thermal initiator after the complete UV curing through the thermal curing.

UV curing behavior, thermal curing behavior and viscoelastic property were investigated sequentially by UV-ARES. Addition of thermal initiator did not affect to storage modulus change in UV curing process. Thermal curing efficiency was decreased as UV dose increased. Especially, the addition of

thermal initiator could not influence the storage modulus after 800 mJ/cm² of UV dose. The results indicated that thermal curing was suppressed by UV curing because the mobility of the polymer was decreased. The thermal curing efficiency was affected to the storage modulus at plateau area. Viscoelastic property results indicated that dual curable adhesives with low UV dose had higher crosslinking density. Adhesion performance was increased due to the formation of network structure with high crosslinking density in low UV dose condition at the shadow area. Based on the result, formation of molecular structure in accordance with dual curing condition was suggested.

Keywords: Adhesive, UV-curing, Dual-curing, Photopolymerization, Adhesion performance, Viscoelastic property, Optically clear adhesives (OCR), Dual curable adhesives, Curing kinetics

Student Number: 2013-23251

Table of contents

Chapter 1

Introduction, Literature Reviews and Objectives 1

1. Introduction 2

1.1. Optically clear resin 2

1.2. Bonding process of touch screen panel 7

1.3. UV curing technology 12

1.4. Dual curing technology 21

2. Literature Review 26

2.1. Curing kinetics 26

2.2. Dual curing technology 29

3. Objectives 33

Chapter 2

Thermal Properties and Adhesion Performance of Dual Curable Adhesives 36

1. Introduction 37

2. Experimental 42

2.1. Materials 42

2.2. Characterization methods 44

2.2.1. Prepolymer synthesis 44

2.2.2. Preparation of adhesive film 44

2.2.3. Fourier transform infrared (FTIR) spectroscopy 45

2.2.4. Gel fraction 45

2.2.5. Thermogravimetric analysis (TGA) 46

2.2.6. Differential scanning calorimetry (DSC) 46

2.2.7. Photo-differential scanning calorimetry (photo-DSC)	46
2.2.8. Adhesion performance	47
2.2.8.1. Peel adhesion	47
2.2.8.2. Probe tack	47
2.2.8.3. Pull-off test	47
3. Results and discussion	49
3.1. Curing behavior of acrylic resin determined by DSC	49
3.2. FT-IR conversion	54
3.3. Gel fraction	59
3.4. Thermal analysis of dual curable adhesives determined by DSC and TGA	62
3.5. Adhesion performance measured by peel strength, probe tack, and pull-off test	67
3.6. Network formation of dual curable adhesives	74
4. Conclusions	78

Chapter 3

Curing Behavior and Viscoelastic Property of Dual Curable Adhesives

1. Introduction	80
2. Experimental	85
2.1. Materials	85
2.2. Characterization methods	87
2.2.1. Synthesis of prepolymer	87
2.2.2. Preparation of adhesive sample	87
2.2.3. Fourier transform infrared (FTIR) spectroscopy	88
2.2.4. Gel fraction	88
2.2.5. Thermogravimetric analysis (TGA)	90
2.2.6. Differential scanning calorimetry (DSC)	90

2.2.7. UV-Advance rheometric expansion system (UV-ARES) analysis	90
3. Results and discussion	91
3.1. Curing behavior of acrylic adhesives determined by DSC and TGA	91
3.2. FT-IR conversion	97
3.3. Gel fraction	99
3.4. Curing behavior and viscoelastic properties determined by UV-ARES	101
4. Conclusions	111
<i>Chapter 4</i>	
Concluding Remarks	112
<i>References</i>	115

List of Tables

Table 1-1. Different type of UV-curable resins	16
Table 2-1. Formulations and operating conditions for dual curable adhesives	40
Table 2-2. Peak heat flow, peak temperature and exothermic area observed via photo-DSC	52
Table 2-3. (a) Thermal decomposition and (b) peak temperature the of DTG curves	66
Table 3-1. Raw materials for synthesis and preparation of optically clear resin	86

List of Figures

Figure 1-1. Global OLED market trends and forecasts	4
Figure 1-2. Construction of touch screen panel	5
Figure 1-3. Difference between air gap structure and OCR structure	6
Figure 1-4. Change in important things in smartphone purchase	6
Figure 1-5. Bonding process of touch screen panel	9
Figure 1-6. Scheme of UV side curing	9
Figure 1-7. Schematic diagram of interruption of the FPCB in the side UV curing process	10
Figure 1-8. Scheme of display bonding process of OCA and OCR	11
Figure 1-9. Main steps of a typical photopolymerization reaction of vinyl compounds	17
Figure 1-10. Oxygen inhibition is radical-induced polymerization	17
Figure 1-11. Scheme of UV curing mechanism	18
Figure 1-12. Chemical structure of multifunctional acrylate monomers	19
Figure 1-13. Illustration of the reaction diffusion process in a cross-linked polymer	20
Figure 1-14. Effect of the addition of a thermal initiator on the hardening process of a dual-cure formulation	23
Figure 1-15. Formation of three-dimensional polymer network by UV irradiation and thermal treatment of a dual curable acrylic- urethane system	24
Figure 1-16. Redox initiation with benzoyl peroxide/amine systems	24
Figure 1-17. Scheme of moisture curing	25
Figure 1-18. Formation of poly-urea linkage by moisture curing	25
Figure 1-19. Thiol conversion and dynamic elastic modulus plotted as a function of the UV exposure time in thiol-ene system	28
Figure 1-20. Photo-DSC exotherms for the photo-polymerization	28
Figure 1-21. Schematic diagram of dual-curing mechanism of dual-curable adhesives	31

Figure 1-22. Dual-cure system after UV and thermal treatment leading to a poly-urethane polyacrylate network in the irradiation and to a polyurethane acrylate network in the shadow area	32
Figure 1-24. Scheme of dual curing under BM area	34
Figure 1-25. Objective of this research	35
Figure 2-1. Preparation and curing process for dual curable adhesives	41
Figure 2-2. Chemical structures of the various compounds used in this study	43
Figure 2-3. Schematic diagram of the assembly for the pull-off test measurements	48
Figure 2-4. (a) UV curing behavior and (b) thermal curing behavior of dual curable adhesives according to the differences in UV dose and TRI content	51
Figure 2-5. Thermal curing behavior at 80°C isothermal condition with different pre-UV dose conditions	53
Figure 2-6. FT-IR spectra of dual cured adhesives with different UV doses and TRI content before and after (a) UV curing and (b) dual curing ..	56
Figure 2-7. FT-IR conversion of the dual cured adhesives with TRI content (a) without a UV dose and with UV doses of (b) 400 mJ/cm ² , (c) 800 mJ/cm ² and (d) 1600 mJ/cm ²	58
Figure 2-8. Gel fraction of the dual cured adhesives with TRI content (a) without a UV dose, and with UV doses of (b) 400 mJ/cm ² , (c) 800 mJ/cm ² and (d) 1600 mJ/cm ²	61
Figure 2-9. Glass transition temperature of the dual cured adhesives measured via DSC after dual curing	64
Figure 2-10. (a) TG and (b) DTG curves of the dual cured adhesives	65
Figure 2-11. Peel strength of the dual cured adhesives with respect to the differences in UV dose and TRI content	69
Figure 2-12. Probe tack of the dual cured adhesives with respect to differences in the UV dose and TRI content	70
Figure 2-13. Pull-off strength of the dual cured adhesives with respect to the differences in the UV dose and TRI content	71

Figure 2-14. Stress-strain curves of the pull-off test for the dual cured adhesives with UV doses of (a) 400 mJ/cm ² , (b) 800 mJ/cm ² and (c) 1600 mJ/cm ²	73
Figure 2-15. Correlation between the network formation and other properties	76
Figure 2-16. Schematic diagram of the network formation of dual curable adhesives	77
Figure 3-1. Free radical generation of (a) photo initiator and (b) thermal initiator	83
Figure 3-2. Synthesis of acrylic prepolymer	84
Figure 3-3. Schematic diagram of gel fraction	89
Figure 3-4. Curing behavior with different initiator contents of (a) acrylic resin, and (c) with UV doses of 400, 800 and 1600 mJ/cm ² . Exothermic peaks of reaction of thermal initiator (b) without UV dose and (d) with UV doses of 400, 800 and 1600 mJ/cm ²	94
Figure 3-5. Thermogravimetric analysis with different initiator contents (a) without UV dose, and with UV doses of (b) 400 mJ/cm ² , (c) 800 mJ/cm ² and (d) 1600 mJ/cm ²	96
Figure 3-6. FT-IR conversion at 810 cm ⁻¹ after dual curing as a function of UV dose and initiator content	98
Figure 3-7. Gel fraction after dual curing as a function of UV dose and initiator content	100
Figure 3-8. Storage modulus of dual curable resin as a function of initiator contents for (a) 0phr, (b) 0.02phr, and (c) 0.1phr with UV curing	104
Figure 3-9. Storage modulus of dual curable resin as a function of initiator contents for (a) 0phr, (b) 0.02phr, and (c) 0.1phr for thermal curing	106
Figure 3-10. Storage modulus of dual curable resin as a function of initiator contents (a) 0phr, (b) 0.02phr and (c) 0.1phr after dual curing for measurement of the viscoelastic properties	108

Figure 3-11. Glass transition temperature of acrylic adhesives measured by
UV-ARES after dual curing 109

Figure 3-12. The effect of UV dose on (a) crosslinking formation and (b)
average molecular weight between crosslinks 110

Chapter 1

Introduction,
Literature Reviews
and Objectives

1. Introduction

1.1. Optically clear resin

Display industry was developed after 1990s from cathode ray tube (CRT) to liquid crystal display (LCD) and plasma display panel (PDP). Now, organic light emitting diodes (OLED) appeared as competing product. OLED is expected to be next generation display by having the availability for application of flexible display or transparent display. The experts have anticipated that the display industries will growth until 2020 as shown in Figure 1-1.

Optically clear resin (OCR) is one of the optical bonding materials which has high refractive index and transmittance for touch screen panel (TSP) and window of the display. Figure 1-2 shows the structure of TSP and window bonding by OCR. The application of optical bonding materials is not only bonding of TSP, but also improving image quality of display by filling up air gap, protecting TSP from external damage and increasing battery efficiency as shown in Figure 1-3. Currently, optical adhesive materials were used in OCA type and OCR type of a form. Although, OCR and OCA have different type of state, they have the same purpose to increase visibility. Figure 1-4 shows the considerations for purchasing the smartphone, and the display is the key factor of smartphone consideration.

OCA is a transparent double-sided adhesive tape. It is possible to apply in the manufacturing process without flow control. But OCA which is solid type adhesive can create bubbles under the adhesive film during the bonding process. Especially, bubbles are easy to be generated near black matrix (BM) area, known as bezel, due to the gap between glass and bezel ink. For that reason, the additional step for removing the bubbles was required. Otherwise, OCR is supplied as a curable resin, and is applied to the bonding process of touch screen panel (TSP) and glass as a resin. Unlike the solid type OCA, the OCR needs delicate process to prevent the overflow while covering the entire

of surface between TSP and glass and for using OCR. Typical disadvantages for OCR are difficulty for process applying, change of resin in the process, the application for flexible display. Additionally, UV curing under BM area causes reliability problem due to the unreacted monomer.

Adhesive materials for optical application demand high transparency for quality improvement, low shrinkage, non-acidic condition for preventing corrosion of TSP and proper viscoelastic property for damping damage. Optically clear adhesives are mainly composed of acrylate, silicone or urethane monomer. The common and widely used siloxane polymers are principally based on poly(dimethylsiloxane) (PDMS). Polyorganosiloxane is consisted of Si-O bond, which shows flexibility of chain, chemical resistance, corrosion resistance, water resistance and thermal, oxidative stability (Lee and Kang, 2007). And polyurethane has been developed greatly because of its excellent mechanical properties, fire resistance, low toxicity and lack of environmental hazard (Xu, Qiu *et al.*, 2012).

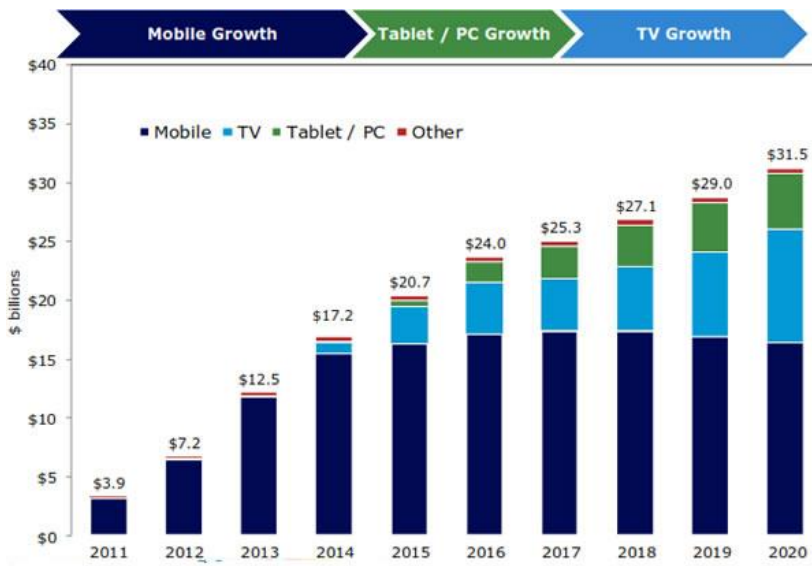


Figure 1-1. Global OLED market trends and forecasts (Display Research, 2012).

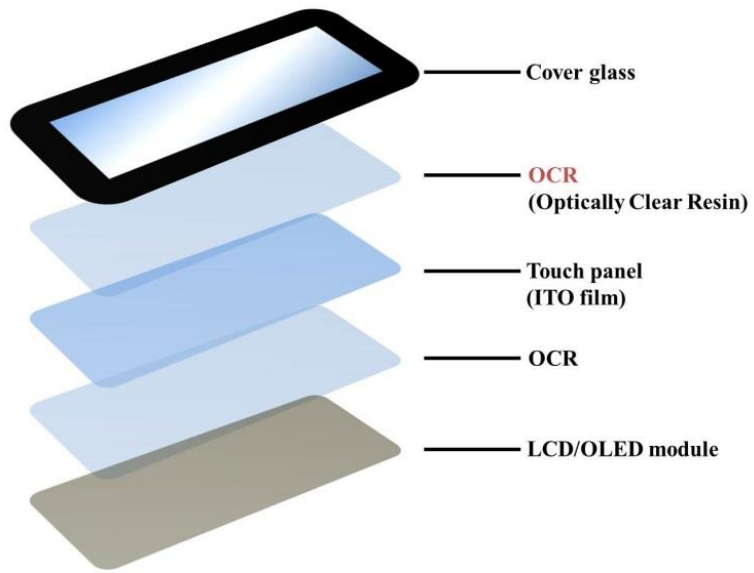


Figure 1-2. Construction of touch screen panel.

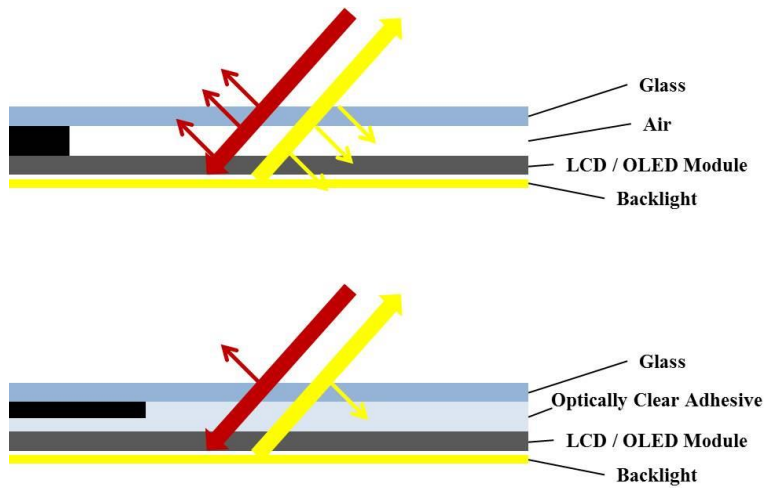


Figure 1-3. Difference between air gap structure and OCR structure (Dexerials Corporation).

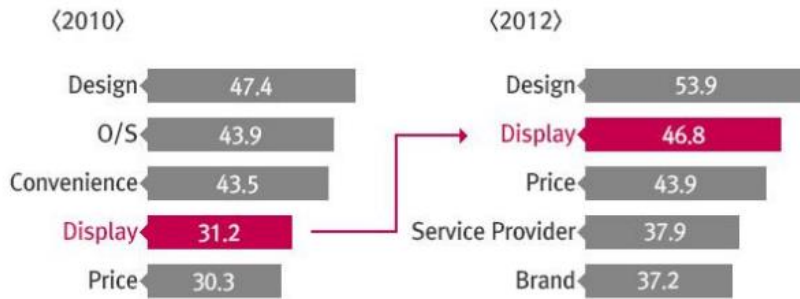


Figure 1-4. Change in important things in smartphone purchase (Korea Communications Commission).

1.2. Bonding process of touch screen panel

UV curing process accomplishes adhesion between touch screen panel (TSP) and OCR. At first, OCR is coated on the glass and combined to TSP. In this step, pre-curing process is treated to the bonded glass and TSP to hold the primary state. And, treating pre-curing process prevents overflow which is the one of main problem in the resin curing process. In the bonding process, various sensors are delicately controlled to coat all over the surface with uniform thickness of adhesive layer between window and panel. After checking the fault such as the bubble inside the adhesive layer or overflow of unreacted resin, TSP and window complex was entered to UV curing chamber for final curing. Figure 1-5 and Figure 1-6 show the bonding process of TSP and window with OCR.

The bonding process with OCA has difference compared with OCR process. In the case of OCA, transparent double-sided tape attaches the window and TSP. The solid type of tape easily causes the bubble inside the window than the liquid. Also, bubble appears between side of the window due to the gap between bezel ink and window. Therefore, the process with OCA requires the vacuum process to remove the bubble. After attaching the process, the attached product is cured inside the UV chamber or oven. The bonding process was shown in Figure 1-8. The process with OCA and OCR are mutual complementary. OCA bonding process was prevalent in the touch panel industry, in the past, due to simple process for application. However, OCR process has specialization in hard to hard adhesion process and easy to control the thickness, while it has complex process for manufacturing.

UV curing process in bonding process can be progressed by two kinds of UV lamps. There are two kinds of UV lamps being currently used, which are the metal halide type UV lamp and the LED type UV lamp. There are two large different points between the metal halide lamp and the LED lamp. Metal halide lamp emits the UV light which have wide range of wavelength distribution. Even when applying to the filter, it has a wide range of light

distribution than that of LED lamp. In addition, temperature of the chamber of metal halide is higher than LED chamber.

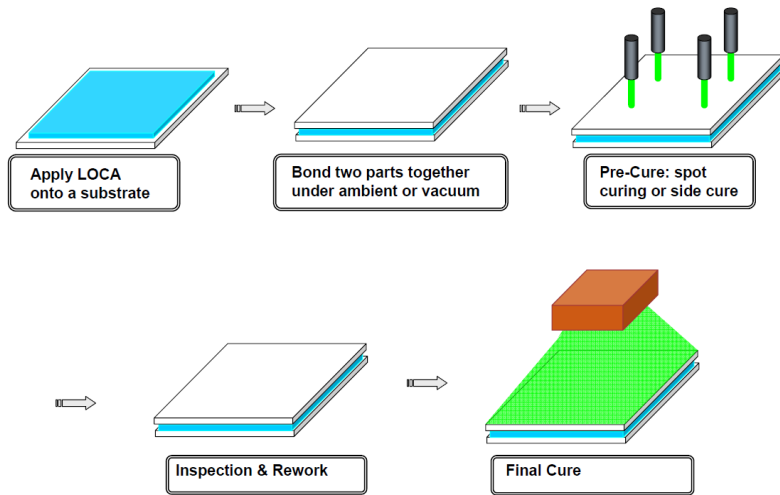


Figure 1-5. Bonding process of touch screen panel (Daniel, 2012).

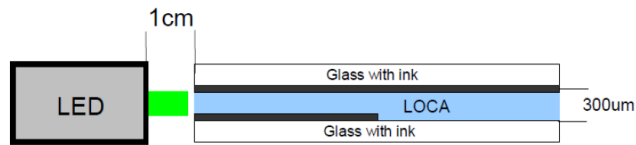


Figure 1-6. Scheme of UV side curing (Daniel, 2012).

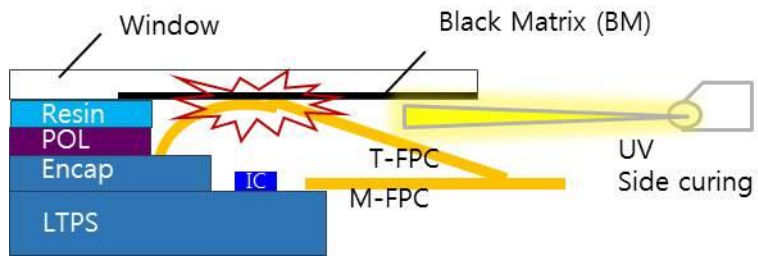


Figure 1-7. Schematic diagram of interruption of the FPCB in the side UV curing process.

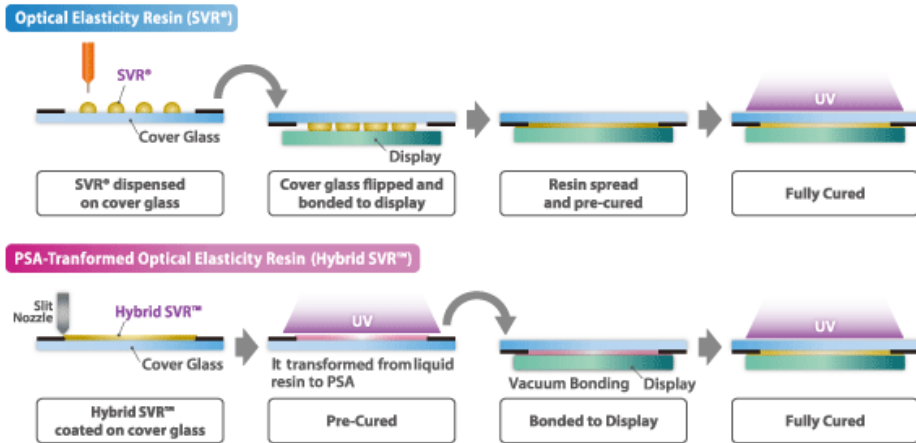


Figure 1-8. Scheme of display bonding process of OCA and OCR (Dexerials Corporation).

1.3. UV curing technology

‘UV curing’ or ‘photopolymerization’ has become a well-accepted technology which has found numerous industrial applications because of its distinct advantages. It is considered to be the most effective way to rapidly transform a solvent-free liquid resin into a solid polymer, at ambient temperature. One of its main characteristics is rapidity of process which quasi-instantly transforms the liquid resin into a solid polymer (Andrzejwska, 2001).

UV curing is rapidly expanding the technology resulting from its main advantages: process is solvent-free, energy efficient and generally economical, spatial and temporal control of polymerization. It has found extensive application for producing photoactive polymer-based systems like coating, paints or printing inks, adhesives, composite materials and dental materials (Scherzer and Decker, 1999). The main interest of using UV-light to induce the polymerization reaction lies in the high polymerization rates, which can be reached under intense illumination, with the advantage of a solvent-free formulation curable at ambient temperature (Decker, Nguyen *et al.*, 2001). Acrylate-based resins are the most widely used light-curable systems because of the high reactivity of the acrylate monomers (Andrzejwska, 2001). Figure 1-9 shows the main steps of photopolymerization.

Today, most research work in UV-initiated photopolymerization has focused on free-radical systems primarily based upon acrylates and methacrylates. Acrylates and methacrylates polymerize rapidly and are easily modified to obtain materials with differing properties (Cho and Hong, 2005). The traditional disadvantages of acrylic photopolymerizations involve oxygen inhibition and use of photoinitiator molecules as shown in Figure 1-10 (Cramer, Scott *et al.*, 2002). The free radicals formed by UV or thermal initiator are rapidly scavenged by oxygen. The by-products by oxygen inhibition are not reactive and cannot participate to polymerization (Studer, Decker *et al.*, 2003). So, free-radically photopolymerizations are inhibited by

oxygen and often must be performed under an inert atmosphere such as nitrogen (Dietliker, 1991).

Relying on the polymerization mechanism, UV curing can be divided into two major class; free radical UV-curing and cationic UV curing. Each of these mechanisms display has benefits and limitations, so both are competitive but complimentary. Cationic UV-initiated photo-polymerizations exhibit several advantages over the free-radical photo-polymerizations. The epoxides and vinyl ethers cured via cationic mechanism are negligibly toxic, are not inhibited by oxygen, exhibit relatively low viscosities, have low shrinkage during curing, and exhibit dark-curing behavior in which the unreacted epoxides and vinyl ethers continue to react slowly upon storage of the sample in the dark after the irradiation has ceased (Cho and Hong, 2005). The monomers using UV or cationic curing are listed in Table 1-1.

Acrylate adhesives are easy to control the balance of adhesion and cohesion by modifying the T_g and the crosslinking density (Czech and Butwin, 2009). Crosslinking is one of the most interesting processes in the application of adhesives. In many applications, adhesives need to have good surface adhesion and stability of external condition. The crosslinking of adhesives is a useful process in the repertoire of general design procedures and is recognized throughout many of the applications of adhesives. In nomenclature used, 'crosslinking' is a correlation of a network, which relates to a net of interconnected chains. Formation of crosslinking is shown in Figure 1-11. Polymer networks or crosslinked systems consist of interconnected macromolecules, which extend into all three dimensions. Individual molecule chains in the crosslinking are interconnected into, effectively infinitely large molecules. Because of the huge length of the starting polymeric chains, only small amount of crosslinking additive are needed to accomplish the complete crosslinking (Czech, 2003).

The application of multifunctional monomer is one of the efficient methods for formation of network polymer (Moussa and Decker, 1993). Typical multifunctional monomers are shown in Figure 1-12. In the

photopolymerization, controlling the functionality of the crosslinking agent modified glass transition temperature of UV curable materials. Because the functionality had the optimum values, it is required to adjust the balance between high conversion and degree of crosslinking with high functionality monomers. Also, photopolymerization has advantage in crosslinking formation with multifunctional monomer due to provision of mobility to the curing system (Anseth, Bowman *et al.*, 1993). Network structure of multifunctional monomer allows the polymer to have thermal stability, mechanical strength and resistance to solvent absorption. Formation of crosslinking by photopolymerization with multifunctional monomers led to increased demand of new application of the materials. So, analysis of curing behavior was required because final properties of the polymer were changed with different crosslinked network formation (Anseth and Quick, 2001). The methods for investigation of curing kinetics measured by photo-differential scanning calorimetry (photo-DSC) and real-time Fourier transform infrared (RT-FTIR) spectroscopy were previously studied to observe the curing behavior with different amount of addition of the monomer, initiator, crosslinking agent and additives (Scherzer and Decker, 1999).

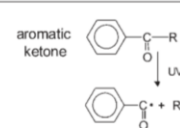
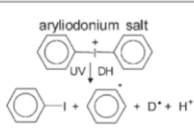
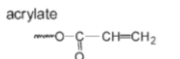
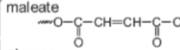
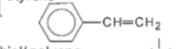
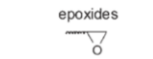
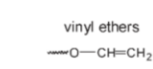
Interpenetrating polymer networks (IPNs) form a special class of polymer blends in which both polymers generally are in network form. IPNs are consisted of intimate combination of two or more polymer in the form of networks in non-chemical linkage between networks. They can be synthesized by crosslinking polymerization of two multifunctional monomers or telechelic oligomers that polymerize by different mechanism, e.g. radical and cationic types (Decker, Nguyen *et al.*, 2001).

Formation of molecular structure was influenced by diffusion limitation. Diffusion limitation affects the curing behavior by autoacceleration, deceleration, trapping of radicals, limited double bond conversion, unequal reactivity of functional groups and volume relaxation effects (Anseth and Quick, 2001). The termination rate was decreased dramatically in a high conversion condition due to the radical trapping. It is indicated that the

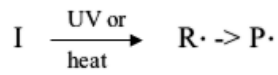
termination rate is decreased as the polymer concentration increases due to the macromolecular chains becoming overlapped and entangled (Zhu, Tian *et al.*, 1990). Autoacceleration was affected to the reactivity by reducing the bulk mobility of the polymer and leading to a diffusion-limited termination mechanism as shown in Figure 1-13 (Anseth, Wang *et al.*, 1994, Lovell, Berchtold *et al.*, 2001).

Also, highly crosslinked polymer can lead to volume relaxation over long periods of time. This volume relaxation was not observed in polymerization of linear or branched polymer or lightly crosslinked polymers. The delay of volume shrinkage affects to increase the maximum attainable conversion. In previous research, the increasing on conversion was observed as the results of increasing on reaction rates, which can be increased by increasing the light intensity and the initiator contents. At the high reaction rate, large volume of polymer during reaction provided higher molecular mobility and faster reaction. As the polymerization proceeds and the network structure are formed, chain mobility becomes restricted. Also, excess volume allows to approaching further reaction and increases the final conversion (Bowman and Peppas, 1991, Anseth and Bowman, 1995).

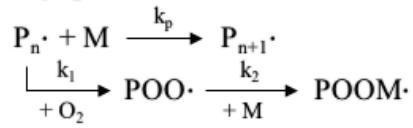
Table 1-1. Different type of UV-curable resins (Decker, 2002).

Mechanism	RADICAL	CATIONIC
Photoinitiator	<p>aromatic ketone</p> 	<p>aryliodonium salt</p> 
Monomers and functionalized polymers	<p>acrylate</p>  <p>maleate</p>  <p>styrene</p>  <p>thiol/ polyene</p> 	<p>epoxides</p>  <p>vinyl ethers</p> 

Initiation



Propagation



Termination

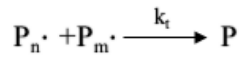


Figure 1-9. Main steps of a typical photopolymerization reaction of vinyl compounds (Bowman and Peppas, 1991).

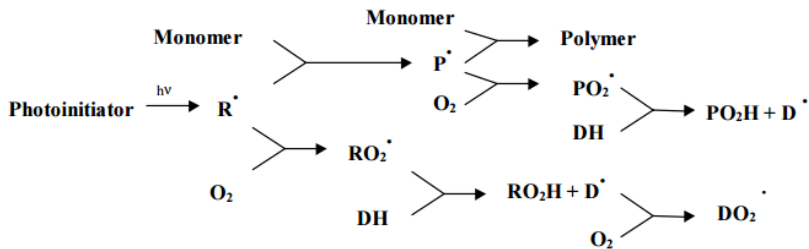


Figure 1-10. Oxygen inhibition is radical-induced polymerization (Studer, Decker *et al.*, 2003).

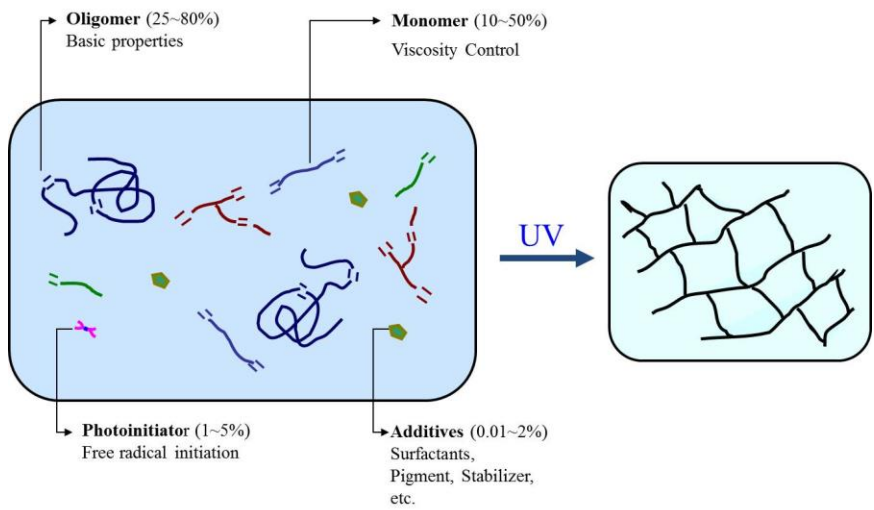


Figure 1-11. Scheme of UV curing mechanism (Kim, Lee *et al.*, 2013).

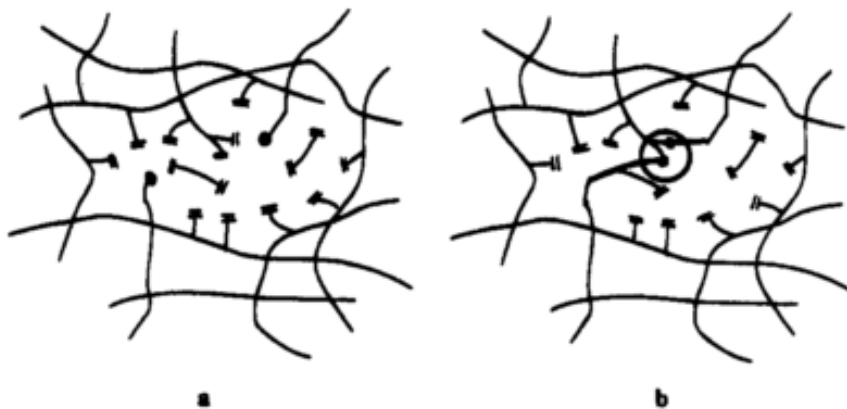


Figure 1-13. Illustration of the reaction diffusion process in a cross-linked polymer (Anseth, Decker *et al.*, 1995).

1.4. Dual curing technology

UV curing has a merit in the manufacturing process due to its various advantages, some examples of its advantages are fast curing rate, low ambient temperature conditions and environmentally friendly. However, UV curing has a limitation of curing on the shadowed area. Especially, OCR coated under a BM area cannot be cured because UV light does not reach to the resin. Therefore, in order to solve the problem, complex curing methods, which is called "dual curing", was applied. In the TSP bonding process, side curing also used with dual curing methods for curing the OCR under the BM area that UV light cannot be radiated. Strictly speaking, side curing is not a dual curing method, but it has been adopted as one of the method for curing under the BM area. Nevertheless, the resin under BM area is not perfectly cured. Therefore, it is required to introduce a dual curing system with UV curing (Daniel, 2012). Figure 1-14 shows the process of dual curing with thermal initiator.

Dual curing means the curing methods that use two different curing methods together in the same material. So, dual curing cannot be defined in specific curing method. Dual curing contains the methods that use different curing sources such as thermal, humidity, UV and EB. Also, it contains the methods that use different reaction conditions of temperature or wavelength. The reason for dual curing to have various methods is to solve the problem that is very particular condition in the process.

The purpose of dual curing application is complementary of conventional methods in aspects of increasing mechanical property, process applicability, and solving problems in the process. For example, dual curing was used in various field such as electrically conductive adhesives (ECA), automobile coating, dental material and chip packaging (Saiki, Kainou *et al.*, 2010). In the ECA or coating application, single UV curing has the limitation for curing shadowed area due to the opaque filler like pigment or silver particle hindering the UV penetration (Studer, Nguyen *et al.*, 2005, Shang, Hao *et al.*,

2015). Also, dual curing can apply to the self-healing coating technology by controlling the curing condition between first and second curing (Hillewaere, Teixeira *et al.*, 2014). In the dental application or hybrid OCA, dual curing is used to provide for facilitating other main curing treatment (Carlborg, Vastesson *et al.*, 2014).

Dual curing was accomplished by various methods combining with different initiators, functional groups or curing sources. Addition of urethane linkage by using isocyanate and alcohol group is typical methods for dual curing by formation of crosslinking with acrylic main polymer or interpenetrating network (IPN) structure as shown in Figure 1-15 (Studer, Decker *et al.*, 2005, Noh, Lee *et al.*, 2012, Park, Hwang *et al.*, 2014). The thiol, thiolene and amine are used for chemical crosslinking between chains. In addition, initiator is used for providing the curability in other curing sources, temperature or wavelength (Xia and Cook, 2003, Hwang, Kim *et al.*, 2013, Carlborg, Vastesson *et al.*, 2014). Heterogeneous monomer condition is used for curing in other curing sources. For example, both epoxy monomer and acrylate monomer are used for curing by UV light and heat, and this method easily forms the IPN structure (Simić, Dunjić *et al.*, 2008, Su, Cheng *et al.*, 2012).

In the display bonding process, curing systems that currently apply with UV curing are thermal curing, moisture curing and redox curing system (Figure 1-16 and Figure 1-17). The dual curing with humidity is accomplished by using isocyanate functional group. The isocyanate group can also undergo curing in a humid atmosphere with formation of ureas crosslinks, even at ambient temperature upon storage of the UV cured coating. But moisture curing of NCO groups in the unexposed areas generates CO₂ and produces bubbles in the crosslinked polymer. Figure 1-18 shows the urea linkage by humidity curing. This is not the case with amines which react even faster with isocyanates. But their potlife time is then so short (a few minutes) which will require some special processing conditions if such systems are to be used in practical applications (Studer, Decker *et al.*, 2005).

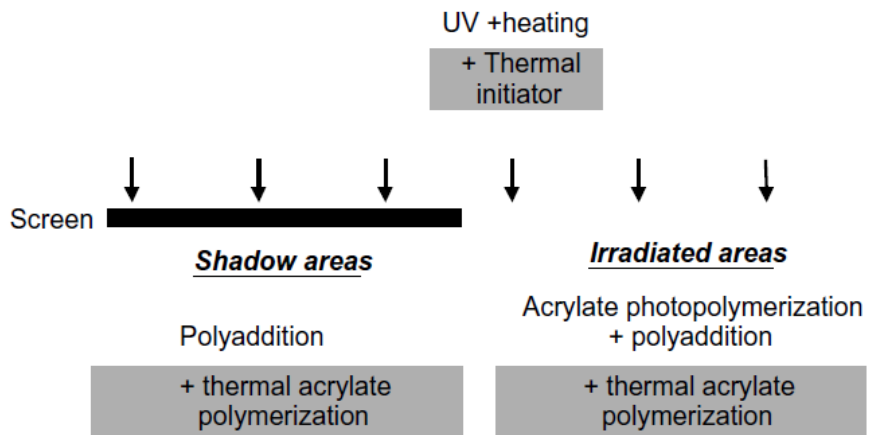


Figure 1-14. Effect of the addition of a thermal initiator on the hardening process of a dual-cure formulation (Studer, Nguyen *et al.*, 2005)

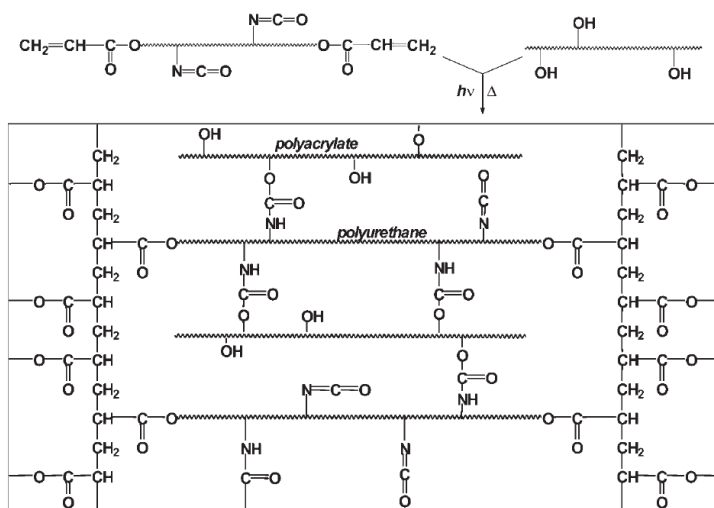


Figure 1-15. Formation of three-dimensional polymer network by UV irradiation and thermal treatment of a dual curable acrylic-urethane system (Decker 2003).

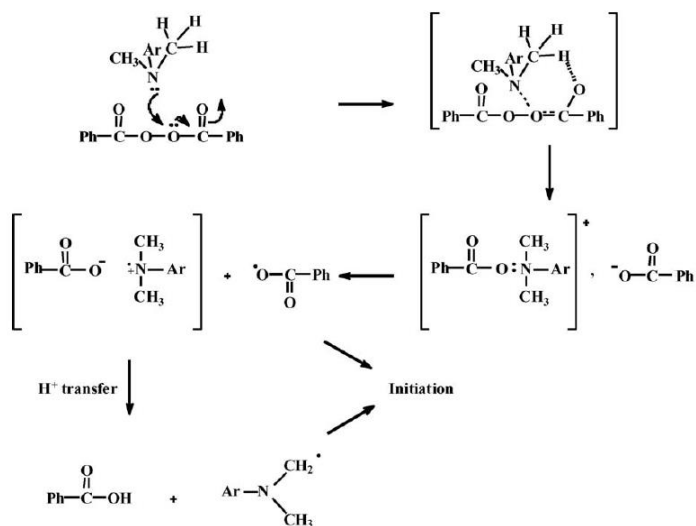


Figure 1-16. Redox initiation with benzoyl peroxide/amine systems (Studer, Nguyen *et al.*, 2005)

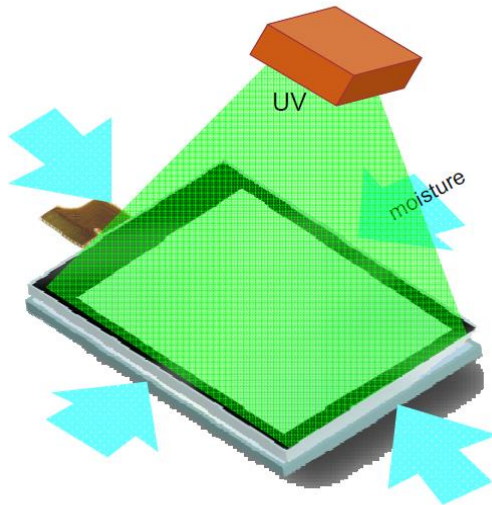


Figure 1-17. Scheme of moisture curing (Daniel, 2012).

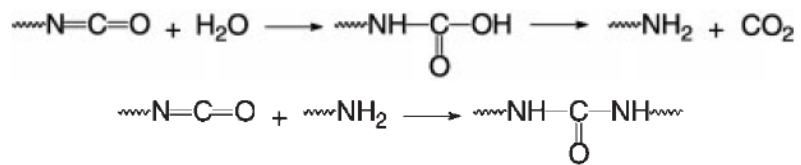


Figure 1-18. Formation of poly-urea linkage by moisture curing (Decker, 2003)

2. Literature Review

2.1. Curing kinetics

Chiou *et al.* reported that the elastic modulus had an appreciable value only when the sample is close to its gel point, consistent with the step growth kinetics of the polymerization reaction. They analyzed UV curing behavior by using real-time FTIR spectroscopy and in situ dynamic rheology of a thiol-ene system containing trimethylolpropane tris(2-mercaptoacetate) and trimethylolpropane diallyl ether. The combination of these two techniques offered a powerful approach for monitoring changes in the chemical and rheological properties of the system during UV curing as shown in Figure 1-19 (Chiou and Khan, 1997).

Scherzer and Decker studied the effect of physical and chemical factors such as photoinitiator concentration, light intensity, temperature, monomer functionality and inertization on kinetic parameters like polymerization rate, induction period and final conversion. The contribution of the pre-curing to the final conversion was determined by following the decay of the double bonds during and after irradiation. Real-Time FTIR-ATR spectroscopy was used to study the kinetics of photopolymerization reactions induced by monochromatic UV light (Scherzer and Decker, 1999).

Cho and Hong reported that photo-curing kinetics analysis using photo-differential scanning calorimetry (photo-DSC) provided utilization to elucidate key cure-process parameters. Figure 1-20 shows the exothermic heat flow by curing of monomers. Photo-DSC was used to investigate the cure kinetics for the UV-initiated cationic photo-polymerization of cycloaliphatic diepoxide (CADE) systems with and without a photo-sensitizer, 2,4-diethylthioxanthone (DETX), in the presence of a diaryliodonium-salt photo-initiator (Cho and Hong, 2005).

Noh et al. reported that The UV–thermal dual-curing procedure improved the crosslinking density and physical properties such as storage modulus, $\tan \delta$, and scratch resistance in comparison with the properties of clearcoats prepared using the thermal–UV dual-curing operation. This improvement is the result of differences in the chain mobility. The dual-curing behavior mainly depended on the optimal reactive functionality induced by the incorporation of hydroxyl groups and the acrylate content. The effects of dual-curing process sequence on the resulting properties of the clearcoats were investigated by controlling the UV dose, the duration of thermal curing, and curing temperature (Noh, Lee *et al.*, 2012).

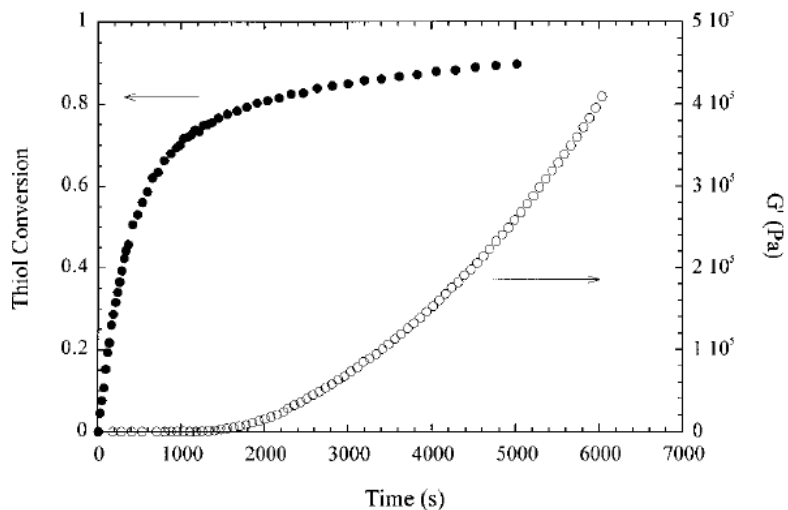


Figure 1-19. Thiol conversion and dynamic elastic modulus plotted as a function of the UV exposure time in thiol-ene system (Chiou and Khan, 1997)

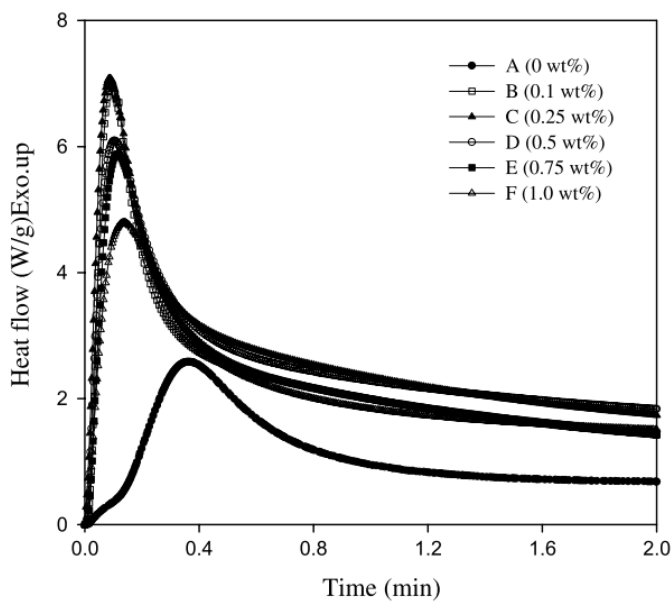


Figure 1-20. Photo-DSC exotherms for the photo-polymerization (Cho and Hong, 2005).

2.2. Dual curing technology

Decker *et al.* reported that the addition of a photosensitizer was shown to speed up substantially the polymerization of the epoxide, with formation within seconds of two fully cured IPNs. IPNs have been synthesized by light-induced crosslinking polymerization of a mixture of acrylate and epoxide monomers. The consumption of each monomer upon UV-irradiation in the presence of radical and cationic-type photoinitiators was monitored in situ by real-time infrared spectroscopy (Decker, Nguyen *et al.*, 2001). Part *et al.* reported that the reaction rate and extent of UV curing were found to be strongly dependent on the concentration of C=C bonds in the epoxy acrylate oligomers. Figure 1-21 shows the scheme of crosslinking formation with dual curing system (Park, Lim *et al.*, 2009).

Studer *et al.* studied that several factors were shown to affect the reaction rate, in particular the chemical structure of the various functionalized compounds, the moisture content in the atmosphere, the curing temperature and the presence of amino catalysts. Figure 1-22 shows the dual curing system of polyurethane acrylate. The viscoelastic properties of the resulting material have been shown to be highly dependent on the curing conditions and the type of polymer network formed (Studer, Decker *et al.*, 2005). Also, studer *et al.* reported that Benzoyl peroxide associated to an amine proved to be a very efficient initiating system to polymerize a typical UV-curable acrylate resin, even at ambient temperature. Because of its short potlife, the formulation has to be utilized as a two-component system prepared just before use. A stable formulation can still be obtained by lowering the initiator concentration down to 0.2 wt.%, but the curing will then require a moderate heating (Studer, Nguyen *et al.*, 2005).

Hwang *et al.* reported that the initial infusion of UV light promoted free radical polymerization during the subsequent thermal curing by generating considerable free radicals in the UV–thermal dual-curing case, and exhibiting a higher growth rate of elastic modulus during the curing in comparison with

the thermal–UV dual-curing case. However, the final modulus value in the thermal–UV dual-curing case was higher due to the suppression of thermal curing by the steric hindrance in the UV–thermal dual-curing (Hwang, Kim *et al.*, 2013).

Shang et al. studied the application of the dual curing system to the electrically conductive adhesives. The electrically conductive adhesives contain the conducting filler such as silver particle which cannot penetrate the UV light. The epoxy resin with thermal curing agent was cured by the heat of the UV lamp. UV-thermal dual curing condition was investigated in accordance with the time of UV curing (Shang, Hao *et al.*, 2015).

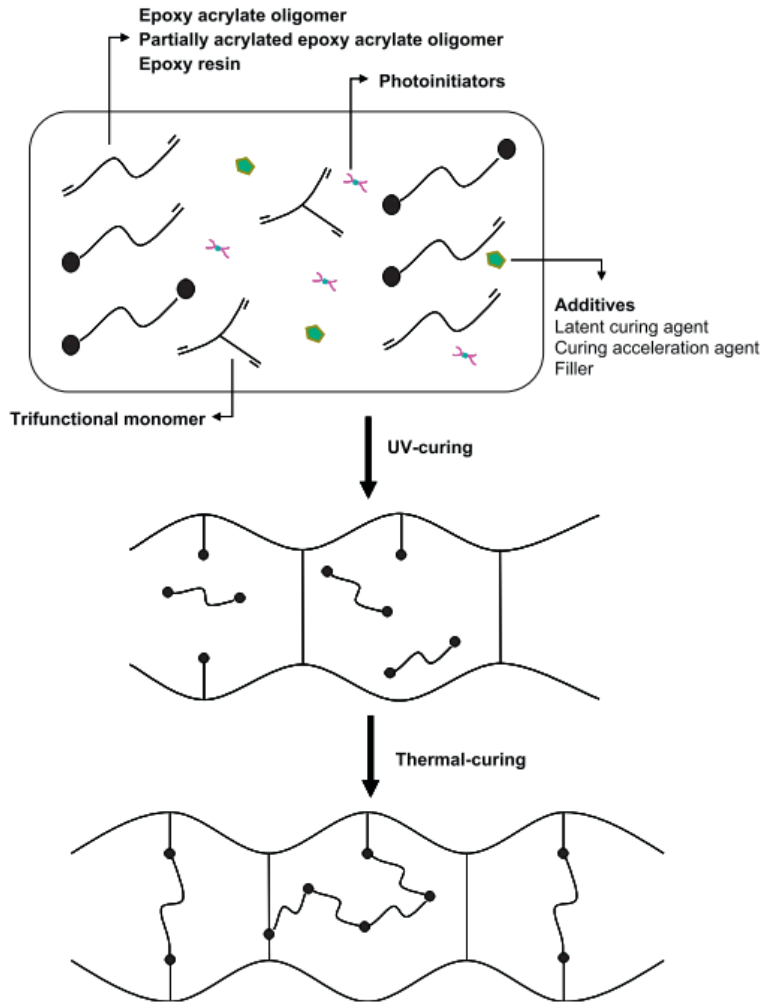


Figure 1-21. Schematic diagram of dual-curing mechanism of dual-curable adhesives (Park, Lim *et al.*, 2009).

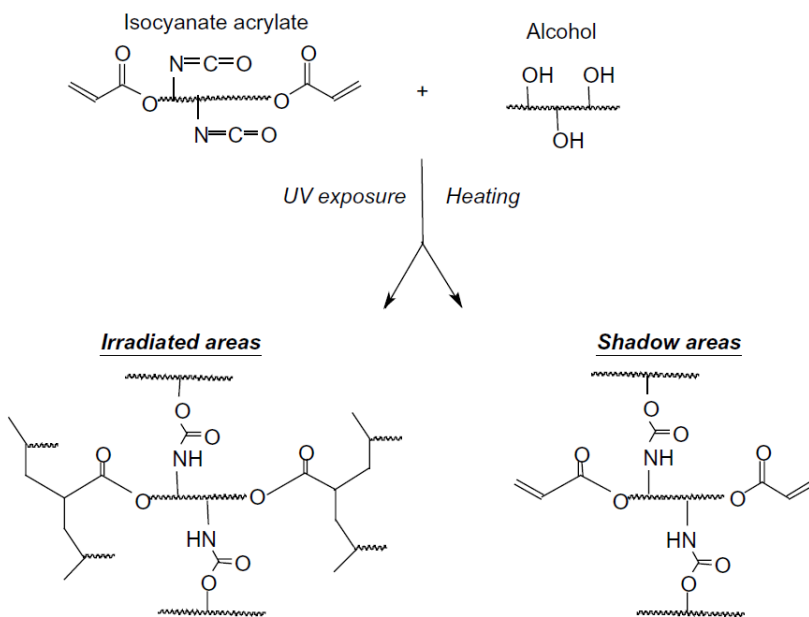


Figure 1-22. Dual-cure system after UV and thermal treatment leading to a poly-urethane polyacrylate network in the irradiation and to a polyurethane acrylate network in the shadow area (Studer, Decker *et al.*, 2005)

3. Objectives

Nevertheless the limitation of UV curing, UV curing is widely used due to the distinct advantages. So, dual curing technics have been developed to broaden the range of applications of UV curing (Studer, Decker *et al.*, 2005). Dual curing system is introduced in many applications for supplement of using one curing method. For example, UV-thermal curing using epoxy monomer or urethane linkage with acrylate is mainly studied in UV-thermal dual curing. However, the previous study has the high curing temperature and remains the unreacted functional groups, because the reaction rate of the urethane linkage or cationic polymerization is lower than that of radical polymerization. The main purpose of this study is the investigation of dual curing behavior with high reactivity thermal radical initiator and effect of initiator contents. Also effect of UV irradiation before thermal curing is observed for application of display bonding process. Figure 1-25 shows the summary of this research.

Transparent part on the glass is not a problem for the sufficient curing using UV light. However, the curing under BM area is not sufficiently cured by UV light because of the hindrance on the light progress. The side curing is used for curing under BM area, but, it is not sufficient methods for curing OCR due to the limitation of penetration of UV light. The curing kinetics with various pre-UV dose conditions is required to analysis due to the randomness of UV irradiation. Also, Viscoelastic property is main factor for determining the adhesion performance. So, change of viscoelastic property of dual curable adhesives is required to analyze depends on UV-curing degree and curing steps. In addition, the network formation is predicted after dual curing in accordance with initiator contents and UV irradiation conditions. It is possible to resolve the curing problems under shadow area in display bonding process without reliability problem and side effect on the current UV-curing process.

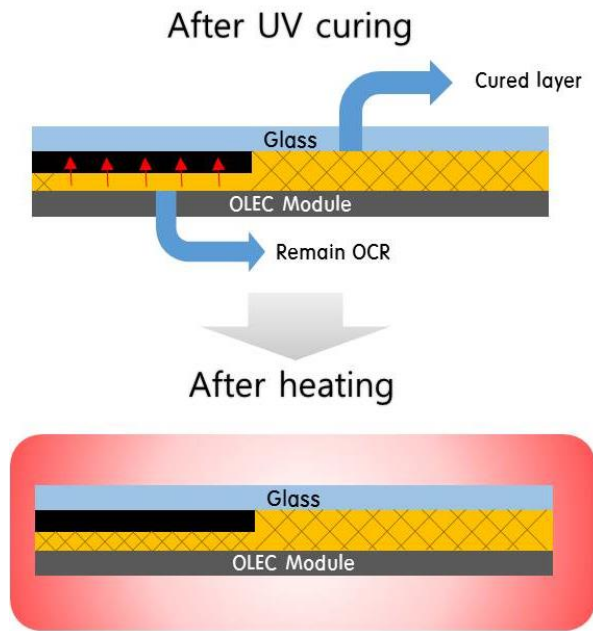


Figure 1-24. Scheme of dual curing under BM area.

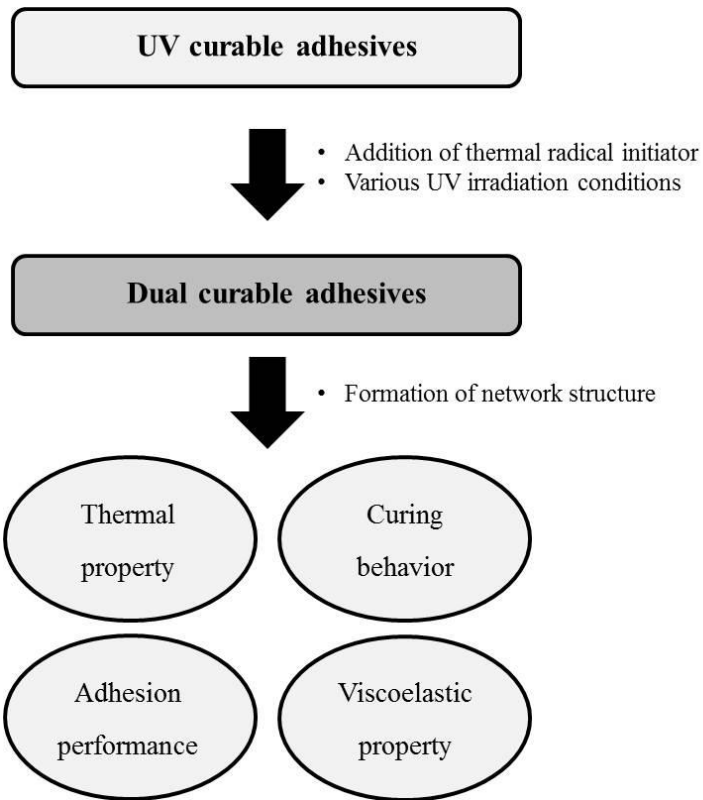


Figure1-25. Objective of this research.

Chapter 2

Thermal Properties and Adhesion Performance of Dual Curable Adhesives

1. Introduction

The display bonding process involves coalescing the window and touch screen panel (TSP) of a device using PSAs or transparent adhesives, such as optically clear resin (OCR) or optically clear adhesive (OCA) (Daniel, 2012, Jang, 2012). The reason to apply OCR or OCA on the entire surface of the display is to bond the TSP and the window and to protect the TSP from an external impact. In addition, this also reduces the loss of light since it minimizes the reflection of light by filling up the air gap between the glass and the panel (Chang, Holguin *et al.*, 2005). The window is divided into two parts: a transparent part of the display and a black matrix (BM) through which light cannot pass. UV light cannot penetrate under the BM area, and so unreacted monomer can cause reliability issues and pollution near the circuit board. The process to simply using light to cure the adhesive is therefore limited in that it cannot be used to cure the shadowed area. A side that is overshadowed by the FPCB does not get cured, even if the devices goes through a side curing process that irradiates light in different directions, as shown in Figure 1-7.

The industry has been increasingly using UV curing because doing so has various advantages including a fast curing speed, low energy consumption, process at room temperature and low VOCs emissions. (Davison, 1999, Decker, Nguyen *et al.*, 2001). In addition, the UV curing process is being considered to replace traditional solvent-borne processes because it is more ecologically friendly and has excellent properties. In particular, acrylate is widely used for the UV radical polymerization because it has a high reactivity (Andrzejwska, 2001). However, the use of a UV curing process has a major disadvantage in that the shaded areas where light cannot reach cannot be cured. For example, the curved portion of an automobile coating and the BM area for a display bonding process cannot be completely cured by only using a UV curing process (Hwang, Kim *et al.*, 2013, Park, Hwang *et al.*, 2014). This

insufficient conversion can result in the elution of materials and can limit of expression of the mechanical properties of the polymer due to the low molecular weight (Eliades, Eliades *et al.*, 1995, Witzel, Calheiros *et al.*, 2005, Kim, Kim *et al.*, 2013).

As a result, various studies have been carried out on dual curing materials that not only respond to a UV curing process but also incorporate other methods of curing. Park *et al.* (Park, Lim *et al.*, 2009) described the dual curing mechanism for epoxy acrylat by forming crosslinking between the hydroxyl group and epoxy group. Studer *et al.* (Studer, Decker *et al.*, 2005) observed the network formation of an acrylic copolymer containing isocyanate and a hydroxyl group in the branch during thermal curing. Hwang *et al.* (Hwang, Kim *et al.*, 2013) studied the dual curing behavior and rheology using a thermal radical initiator for automotovie applications. Shan *et al.* (Shang, Hao *et al.*, 2015) explored the application of a UV-thermal dual curing system for electrically conductive adhesives (ECAs).

In this study, 2,2'-Azobis (4-methoxy-2,4-dimethyl valeronitrile), which has a 30°C half-life decomposition temperature (HLT), was used with acrylic prepolymer, photo radical initiator and a crosslinking agent. An initiator with a low HLT was used because the touch screen panel could be damaged at a high temperature during thermal curing, and it was also used to make it possible to cure the material with the ambient temperature of the metal halide UV lamp chamber. A minimum amount of initiator was added because the resin becomes unstable as excessive TRI is added, and other problems may occur, such as self-curing, undissolving and yellowing during storage. In previous studies, adding more than 0.2phr of the initiators resulted in an unstable state (Studer, Nguyen *et al.*, 2005). On the other hand, a photo radical initiator was added in a sufficient amount to cure the shadowed area during side curing with a low UV dose and to reduce the process time as much as possible. During the process, the dual curing behavior was measured with UV doses of 0, 400, 800 and 1600m J/cm² because curing can proceed in a variety of pre-UV curing conditions due to the randomness of the UV

penetration. Table 2-1 provides the sample name of each of the dual cured adhesives. Isobornyl acrylate, 2-ethylhexyl acrylate, and N-vinyl caprolactam were used as monomer. Poly(ethylene glycol (200) dimethacrylate) was used as a crosslinking agent. Figure 2-1 shows the brief procedure to prepare the sample. Then, FT-IR was used to investigate the chemical reactions within the adhesive. The formation of a cross-linked structure was evaluated through a gel fraction. The curing behavior was also evaluated via DSC and TGA, and peel strength, probe tack and pull-off tests were conducted to assess the adhesion strength.

Table 2-1. Formulations and operating conditions for dual curable adhesives.

Name	UV dose (mJ/cm ²)	TRI contents (phr)
DCA-0000		0
DCA-0002	0	0.02
DCA-0005		0.05
DCA-0010		0.1
DCA-0400		0
DCA-0402	400	0.02
DCA-0405		0.05
DCA-0410		0.1
DCA-0800		0
DCA-0802	800	0.02
DCA-0805		0.05
DCA-0810		0.1
DCA-1600		0
DCA-1602	1600	0.02
DCA-1605		0.05
DCA-1610		0.1

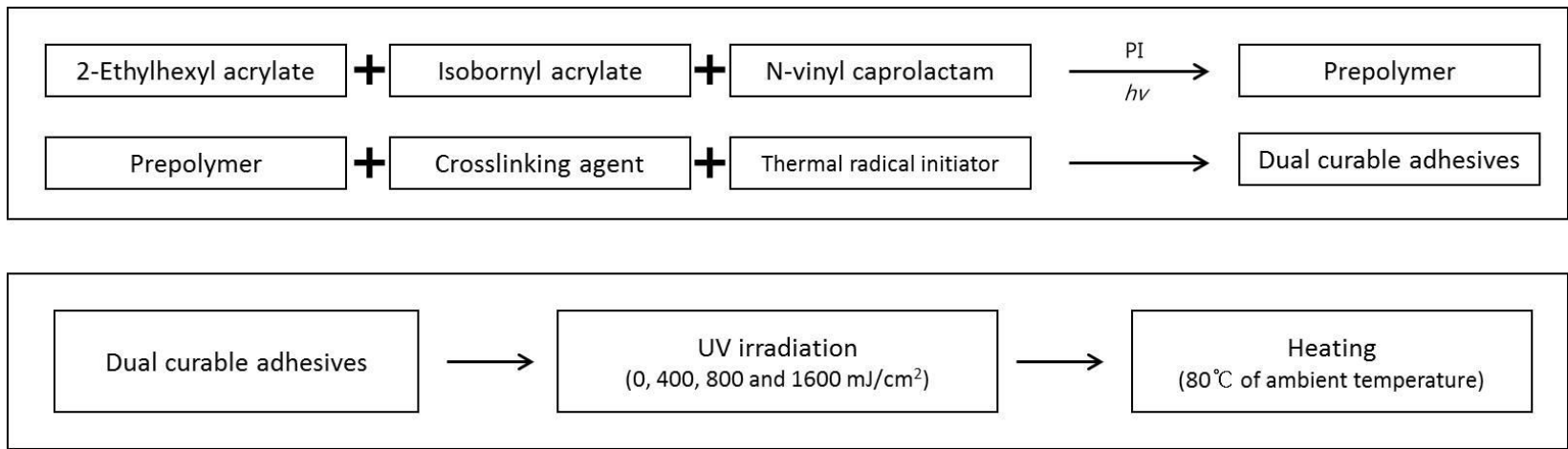


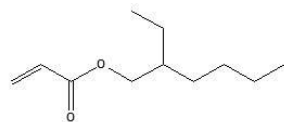
Figure 2-1. Preparation and curing process for dual curable adhesives.

2. Experimental

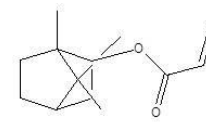
2.1. Materials

2-Ethylhexyl acrylate (2-EHA, Sigma Aldrich, USA), isobornyl acrylate (IBA, Sigma Aldrich, USA) and N-vinyl caprolactam (VC, Tokyo Chemical Industry, Japan) were used as monomers. Poly(ethylene glycol (200) dimethacrylate) (PEGDMA 200, Miwon Specialty Chemical, Republic of Korea) was used as a difunctional monomer to produce the network structure in the adhesives. Hydroxydimethyl acetophenone (Micure HP-8, Miwon Specialty Chemical, Republic of Korea) was used as a photo radical initiator. 2,2'-Azobis(4-methoxy-2,4-dimethyl valeronitrile) (V-70, Wako Pure Chemical Industries, Japan) was used as the thermal radical initiator. All reagents were used without any further purification. The chemical structures of each monomer and initiator are shown in Figure 2-2.

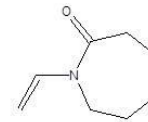
Monomer



2-Ethylhexyl acrylate

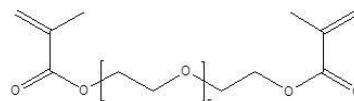


Isobornyl acrylate



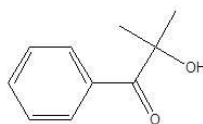
N-vinyl caprolactam

Crosslinking agent

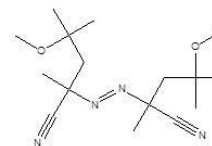


Poly(ethylene glycol (200) dimethacrylate)

Initiator



Hydroxy dimethyl acetophenone



2,2'-Azobis(4-methoxy-2,4-dimethyl valeronitrile)

Figure 2-2. Chemical structures of the various compounds used in this study.

2.2. Characterization methods

2.2.1. Prepolymer synthesis

The prepolymer was prepared using 2-EHA, IBA and VC via bulk radical polymerization under UV irradiation with 1 wt.% of photo radical initiator. Polymerization was performed in a 500 ml four-necked rounded-bottomed flask equipped with a mechanical stirrer, N₂ inlet, thermometer and LED UV lamp. The temperature will be maintained at room temperature with constant stirring with 100 rpm. After N₂ is purged for 30 min with constant stirring, the monomer mixtures were exposed using a UV lamp with 20 mW/cm² of UV intensity for 70 seconds under N₂ purging (Kim, Lee *et al.*, 2013).

2.2.2. Preparation of adhesive film

The dual curable adhesives were prepared by blending prepolymer with 1phr of crosslinking agent and thermal radical initiator. The mixture was mixed with a paste mixer at 600 rpm and 500 rpm for 3 min. The acrylic resin was coated to a 100 μm thickness on corona-treated polyethylene terephthalate films (PET, SKC Co. LTD., Republic of Korea). The coated resin was cured by UV curing using a UV conveyor equipped with medium pressure mercury UV-lamps with an intensity of 154 mW/cm² and main wavelength of 365 nm. The irradiated UV doses were of 200, 400, 800 and 1600 mJ/cm². The UV doses were measured using an UV radiometer (IL 390C Light Bug, International Light Inc.). Each of the pre-cured adhesives with various curing degrees was cured in the oven at 80°C for 5, 10 and 30 min.

2.2.3. Fourier transform infrared spectroscopy (FT-IR)

The IR spectra of the samples were observed using Fourier-transform infrared spectrometry (JASCO FTIR-6100) equipped with an attenuated total reflectance (ATR) accessory. The spectra were collected with 32 scans at a resolution of 4 cm⁻¹ between 4000 and 400 cm⁻¹. The acrylate double bond conversion was calculated using following equation:

$$\text{Conversion (\%)} = \frac{(A_{810})_0 / (A_{1720})_0 - (A_{810}) / (A_{1720})}{(A_{810})_0 / (A_{1720})_0} \times 100 \quad (1)$$

where $(A_{810})_0$ is the intensity for 810 cm⁻¹ at the initial time and (A_{810}) is the intensity for 810 cm⁻¹ after curing.

2.2.4. Gel fraction

The gel fraction of the dual curable adhesives after UV curing and thermal curing was determined by soaking the samples in toluene for 1 day at room temperature. The amounts of the sample were about 0.2-0.3 g. In addition, the insoluble part of the adhesives was filtered with a 40 mesh net and dried at 70°C oven. The gel fraction was calculated by applying the following equation:

$$\text{Gel fraction (\%)} = (W_1 / W_0) \times 100 \quad (2)$$

where W_0 is the weight before filtration, and W_1 is the weight after filtration. The test was replicated five times.

2.2.5. Thermogravimetric analysis (TGA)

TGA measurements were carried out using a thermogravimetric analyzer (TGA 4000, PerkinElmer, USA). The samples of 7–10 mg were evaluated from 50 to 400°C at a heating rate of 5 °C/min. During the test, the dual cured adhesives and the resin were placed in an inert nitrogen atmosphere (99.5% nitrogen, 0.5% oxygen content) to prevent unwanted oxidation.

2.2.6. Differential scanning calorimetry (DSC)

Differential scanning calorimetry (DSC) measurements were carried out using a TA Q200 differential scanning calorimeter with a scanning temperature ranging from -50 to 200°C at a scanning rate of 2 °C/min with an isothermal test at 80°C for 30 min. The analysis was carried out with samples of 7–8 mg each. Each sample was scanned in the dynamic mode and was cooled at the same rate under a nitrogen atmosphere. The thermal curing behavior was determined from the first scan. The glass transition temperature (T_g) was determined during the second scan.

2.2.7. Photo-differential scanning calorimetry (photo-DSC)

Photo-DSC measurements were taken using a TA Q200 differential scanning calorimeter equipped with a UV irradiation accessory (Omniscure 2000) that used UV light from a 100W middle-pressure mercury lamp with a range in wavelength from 300 to 400 nm. The UV light level of the UV accessory with a 90% UV filter was of 10. The analysis was carried out for samples of 1.5–2 mg in an open aluminum DSC pan. After UV irradiation, the thermal curing behavior was determined as the scanning temperature range from 30 to 80°C at a scanning rate of 2 °C/min.

2.2.8. Adhesion performance

2.2.8.1. Peel adhesion

The acrylic adhesive films that were prepared were attached to a stainless steel substrate, and a 2 kg rubber roller was passed over them twice. The 180° peel strength was measured using a Texture Analyzer (TA-XT2i, Micro Stable Systems, UK) after the sample had been left to stand at room temperature for 24 hours. The peeling speed was of 300 mm/min, and the average strength of the peeling period was measured 5 times.

2.2.8.2. Probe tack

A debonding speed of 0.5 mm/sec was maintained on the surface of the adhesives for 1 sec under a constant force of 100 g/cm², and the probe tack was measured as the maximum debonding force. The tack measurements of the adhesive films were carried out with a TA-XT2i Texture Analyzer (Micro Stable Systems, UK) at 25°C using a probe tack consisting of a polished stainless steel (type 304) cylinder probe with a diameter of 5 mm.

2.2.8.3. Pull-off test

On the glass surface, the dual-curable adhesives were loaded and crosswise covered with the slide glass (75×25×1 mm³), as portrayed in Figure 2-3. These assemblies were cured using UV-curing equipment with a 100-W high-pressure mercury lamp (Main wavelength of 340 nm). The UV dose was of 0, 400, 800 and 1600 mJ/cm². The UV doses were measured with an IL 390C Light Bug UV radiometer (International Light, Inc., USA). Next, the UV-cured assemblies were cured in a drying oven for 30 min at 80°C. The measurements of the adhesion strength were performed at room temperature with a crosshead speed of 2 mm/min.

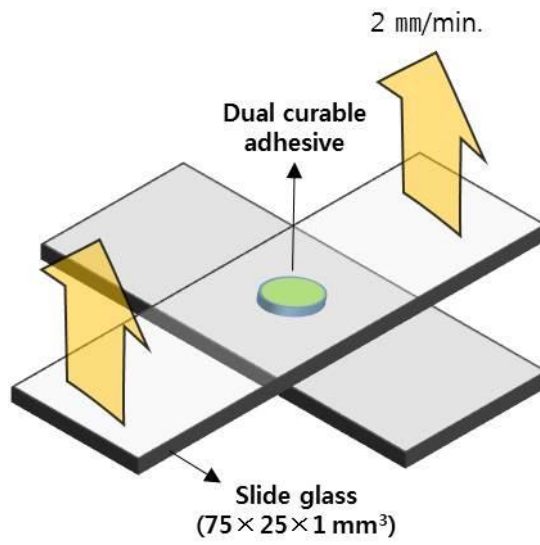


Figure 2-3. Schematic diagram of the assembly for the pull-off test measurements.

3. Results & Discussion

3.1. Curing behavior of acrylic resin determined by DSC

The DSC and photo-DSC are a form of thermal analysis that provides the curing kinetics of the polymerization of the dual curable adhesives. The polymerization of the acrylic resin is achieved through the destruction of the C=C bond, and the reaction of the monomer and the kinetics are analyzed by measuring the heat flow (Nelson, Jacobs *et al.*, 1995 and Boey, Rath *et al.*, 2002). It is not easy to evaluate the UV-curing behavior because the UV-curing process is very fast. In this respect, photo-DSC is an adequate evaluation method that can be used to analyze the UV curing behavior. The reactivity of the acrylic resin is assessed by plotting the heat flow against time and temperature in order to describe the UV curing and thermal curing behavior.

Figures. 2-4a and 2-4b show the UV curing behavior and the thermal curing behavior after UV irradiation as the initiator content changed. In Figure 2-4a, the UV curing behavior is evaluated through UV irradiation each for 0, 6, 60 seconds through the use of a metal halide lamp in photo-DSC. As shown in Table 2-2, the integration area was 0.85 J/g for 6 seconds, and the area was 4.4 J/g for 60 seconds. The 6-second curing time was set to have a 20% curing level for the 60 seconds cure time. Even when the content of the thermal initiator increases, the UV curing behavior is not affected, so no change is found for the peak time and the exothermic area. Figure 2-5 shows the thermal curing behavior of the residual monomer through a temperature scan after UV irradiation. When the initiator content increased from 0.02phr to 0.1phr, the reactivity for the thermal curing became accelerated. This can be found on the graph where the starting temperature increases 10.4°C with 0 sec of UV irradiation and increases 9.5°C with 6 sec of irradiation. In addition, the exothermic peak of the thermal curing decreases as the UV irradiation

increases for the 0.1phr TRI contents, but the same amount of 68 J/g were released for both the 0 sec and 6 sec UV irradiation conditions with 0.02phr of TRI content. This is because the amount of reaction for the 0.1phr of TRI decreased by exhausting the monomers as the UV curing progressed. However, a sufficient amount of remaining monomer can be cured without a reduction of the reactivity at 0.02phr of thermal initiator.

In Figure 2-5, the adhesive films (DCA-0010, DCA-0410 and DCA-1610) that were irradiated with UV doses of 0, 400 and 1600 mJ/cm² in a UV conveyor show a curing behavior at 80°C in isothermal conditions. When the curing behavior of the three adhesive films was checked, the peak height decreased as the UV dose increased in the following order: DCA-0010, DCA-0410 and DCA-1610. A comparison of the samples without UV irradiation shows that the thermal curing peak rapidly forms at DCA-0410, but the reactivity rather decreases at DCA-1610. Therefore, the photo-DSC and DSC results indicate that UV curing rarely is affected even if TRI is being added, and when TRI content increases, the reaction peak shifts to a lower temperature. In addition, thermal curing suppression is not affected with a small amount of UV irradiation, but the thermal curing is suppressed when UV curing sufficiently progresses.

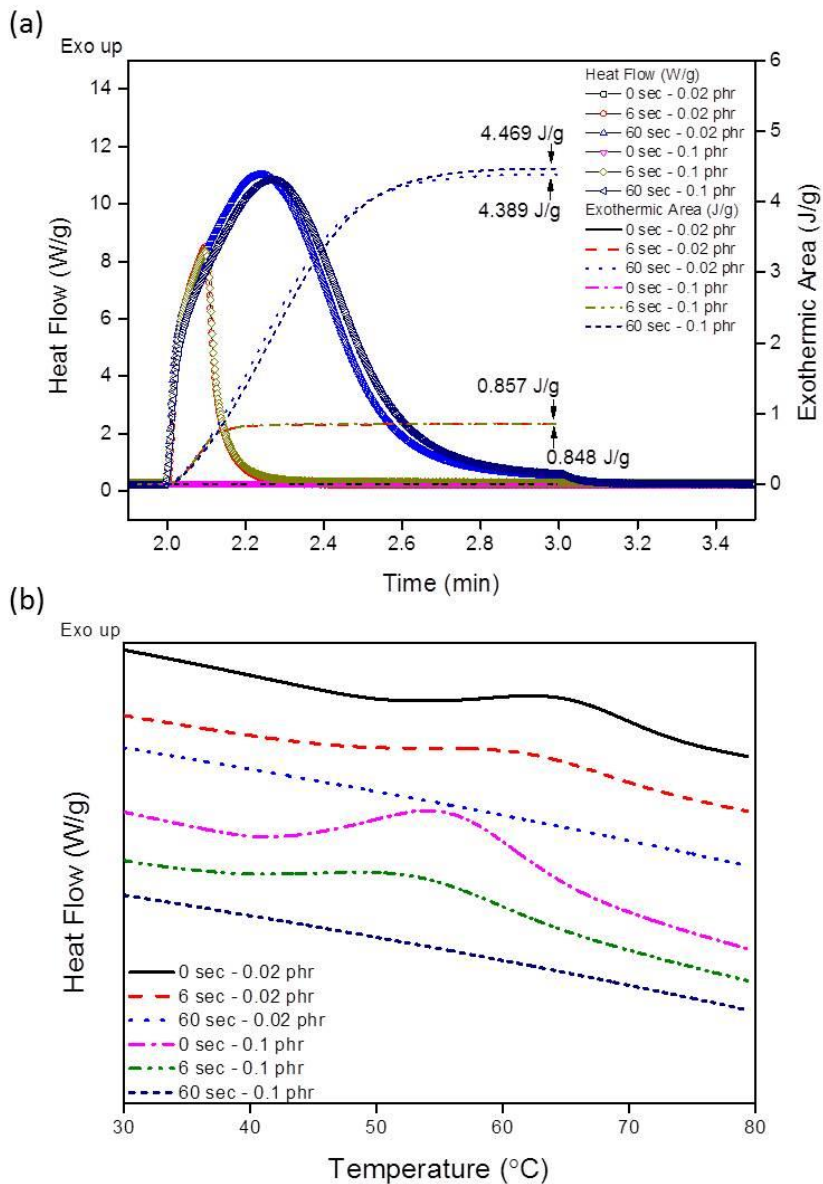


Figure 2-4. (a) UV curing behavior and (b) thermal curing behavior of dual curable adhesives according to the differences in UV dose and TRI content.

Table 2-2. Peak heat flow, peak temperature and exothermic area observed via photo-DSC.

UV curing time (sec)	Initiator contents (phr)	UV curing		Thermal curing		
		Maximum heat flow (W/g)	Exothermic area (J/g)	Starting temperature (°C)	Peak temperature (°C)	Exothermic area (J/g)
0	0.02	-	-	52.5	64.5	68.1
	0.1	-	-	42.1	55.6	195.9
6	0.02	8.49	0.85	46.6	61.4	68.6
	0.1	8.36	0.86	37.1	53.3	125.1
60	0.02	11.02	4.39	-	-	-
	0.1	10.85	4.47	-	-	-

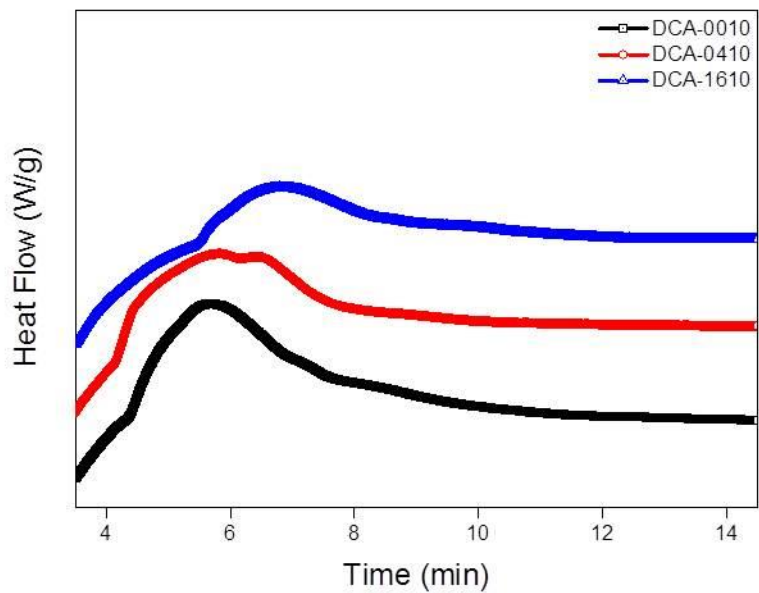


Figure 2-5. Thermal curing behavior at 80°C isothermal condition with different pre-UV dose conditions.

3.2. FT-IR conversion

The change in the chemical bond during polymerization of the acrylic resin was evaluated via FT-IR ATR spectroscopy. The amount of reaction can be measured via FT-IR because the C=C bond of the acrylic resin was consumed during polymerization. Figure 2-6a shows the FT-IR spectra after UV irradiation of the acrylic resin of 0, 400, 800 and 1600 mJ/cm². The 1410 cm⁻¹ peak of vinyl C-H in the plane bend and 810 cm⁻¹ peak of the C=C bond were reduced depending on the UV curing progress. In addition, the 1680 cm⁻¹ peak for amide decreased, and the peak of the secondary C-N amine bond increased. The change in the amine peak was caused by a reaction of the N-vinyl caprolactam. This result confirms that the lactam ring of N-vinyl caprolactam opened as the reaction proceeded and was converted to secondary amine. Equation (1) can be used to calculate the conversion as 25% with 400 mJ/cm², 70% with 800 mJ/cm² and 99% with 1600 mJ/cm² UV dose without heating.

Figure 2-6b shows the change in the FT-IR spectra during the dual curing process after irradiation with 400 mJ/cm² UV dose. A comparison of the peaks of DCA-0402 with DCA-0410 indicates that DCA-0402 had a higher absorbance peak at wavelength of 810 cm⁻¹ because the small amount of initiator was not enough for the reaction to produce enough radical. In addition, the amide peak decreased, the secondary amine peak increased, and the chemical changes were observed to be similar to those of adhesives cured only with UV light even though dual curing was performed with a low UV dose.

As shown in Figure 2-7, the conversion was used to evaluate the curing behavior with various UV doses during the UV-thermal dual curing process. When the UV dose increased, the reactivity of the thermal curing was accelerated, but the dual curable adhesives with TRI content of less than 0.1phr cannot generate sufficient radical to ensure sufficient conversion. Figure 2-7a shows the change in the conversion with different initiator content without UV irradiation sample. For the 10 min curing time, the conversion did

not change for all initiator contents. As previously mentioned, the conversion at a 30 min curing time indicates insufficient conversion when using a low level of initiator content. However, Figures. 2-7b and 2-7c show that thermal curing was observed at 10 min, which indicates that thermal curing accelerated, as shown in Figure 2-4. However, Figure 2-7d shows the change in the conversion that rarely occurred due to the exhausted C=C bond resulting from UV irradiation at 1600 mJ/cm².

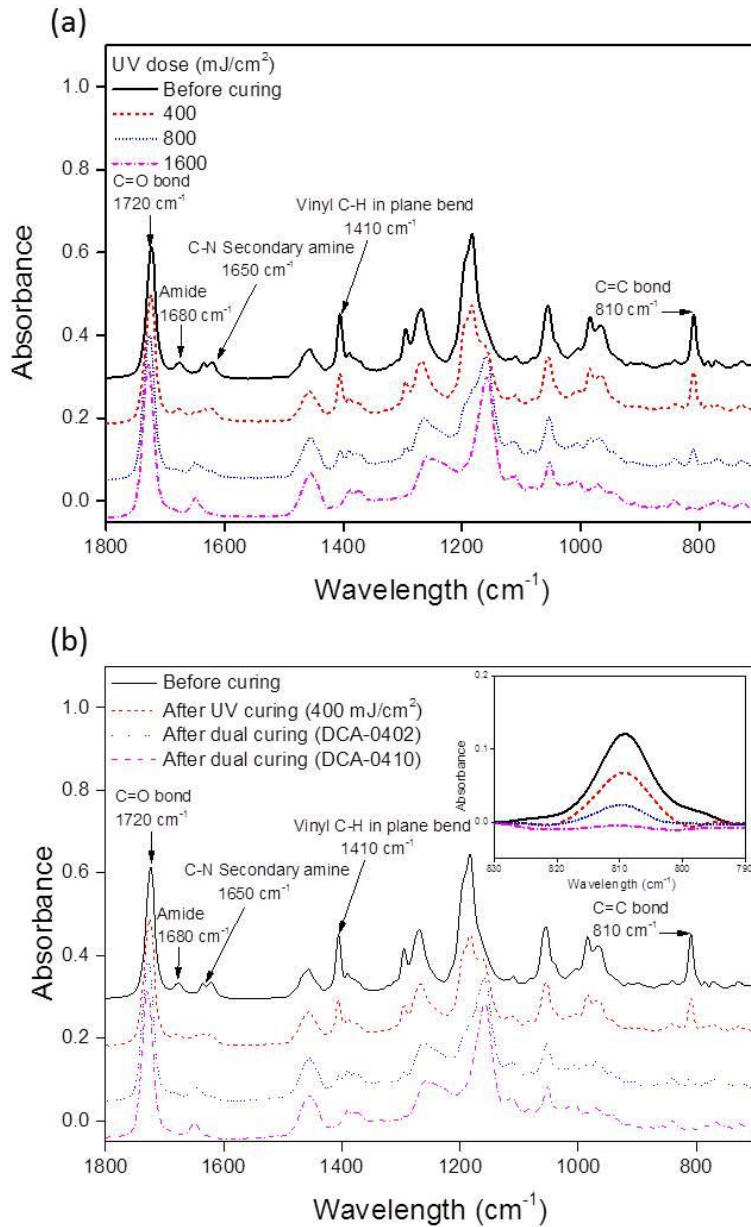
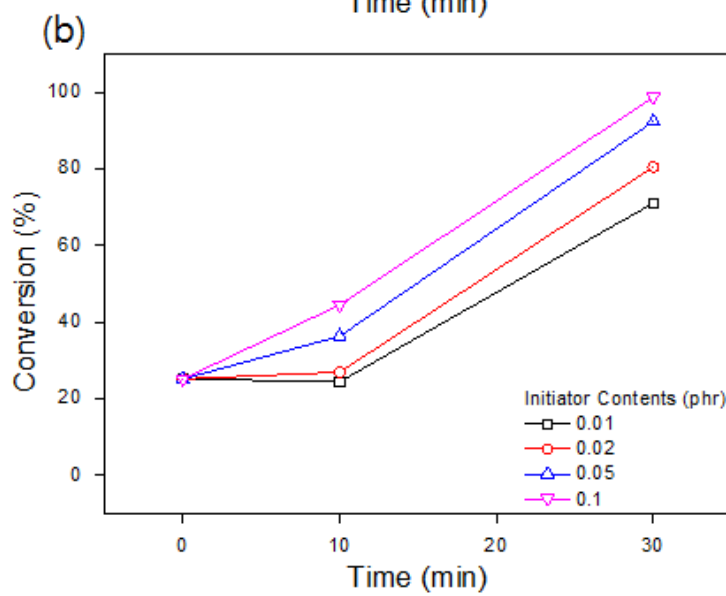
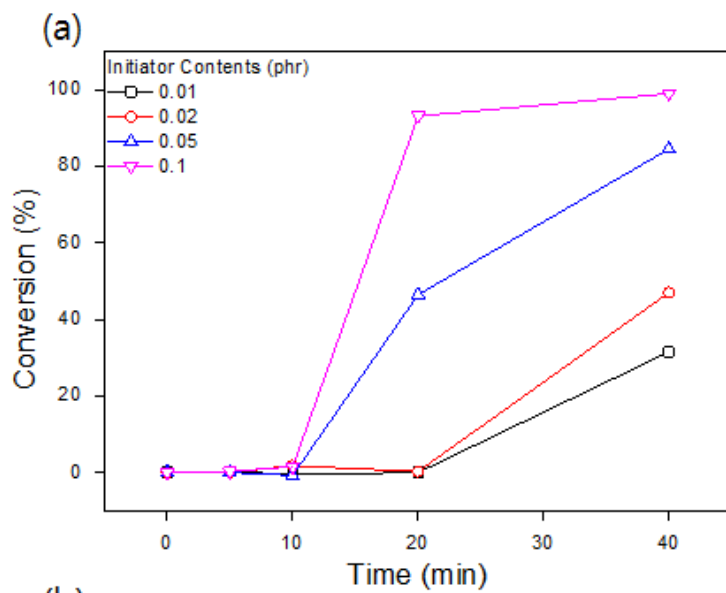


Figure 2-6. FT-IR spectra of dual cured adhesives with different UV doses and TRI content before and after (a) UV curing and (b) dual curing.



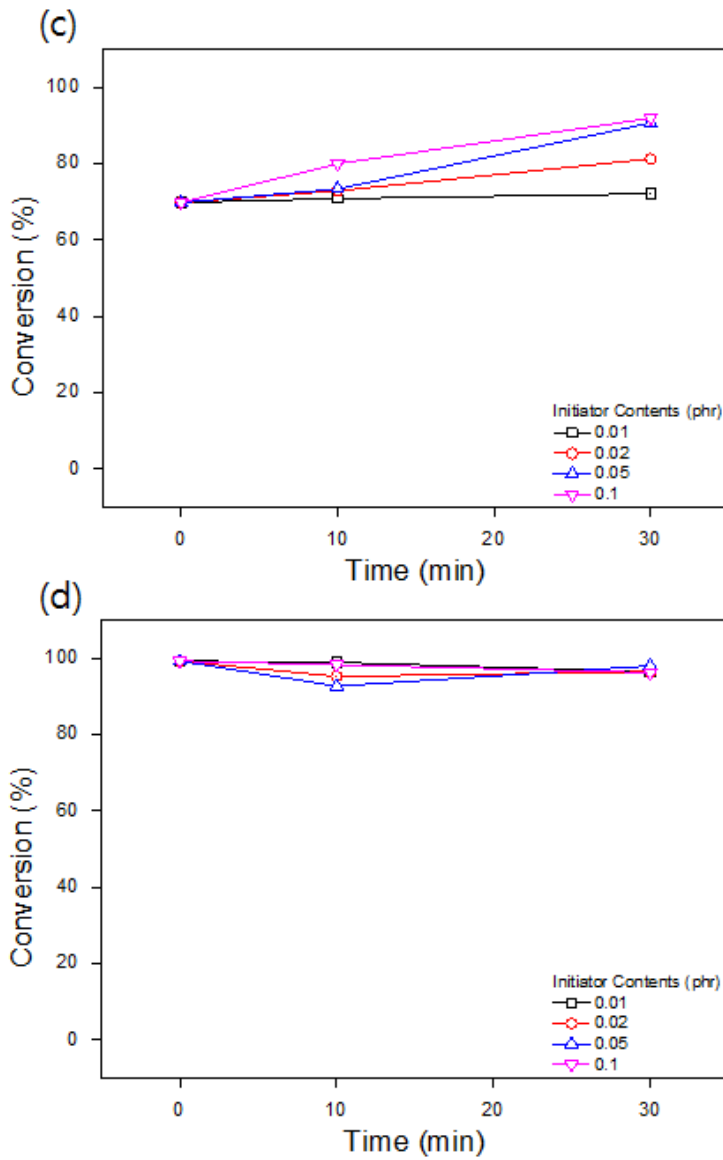
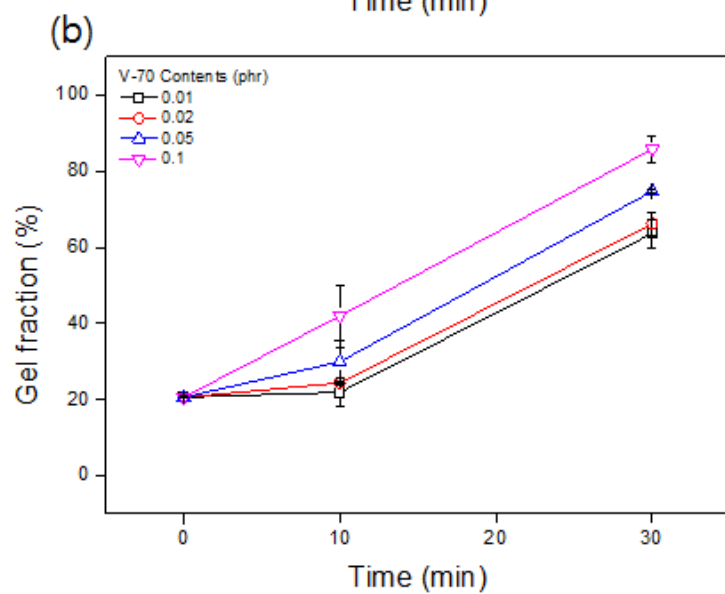
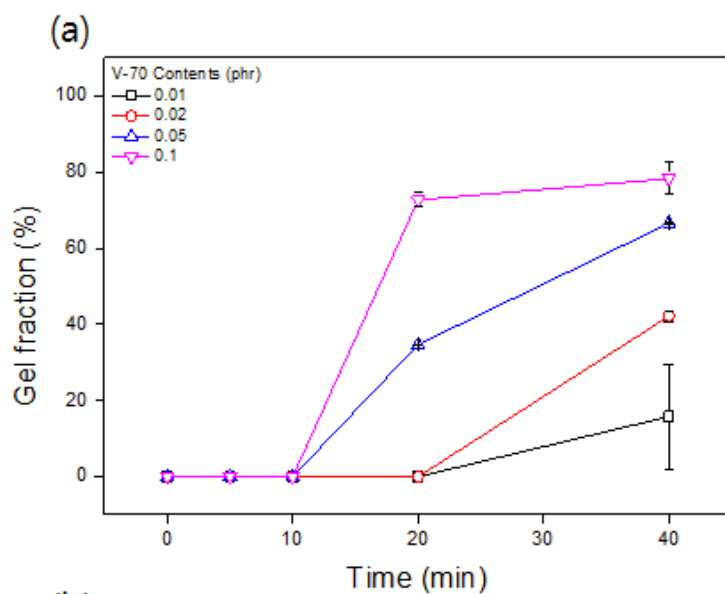


Figure 2-7. FT-IR conversion of the dual cured adhesives with TRI content (a) without a UV dose and with UV doses of (b) 400 mJ/cm², (c) 800 mJ/cm² and (d) 1600 mJ/cm².

3.3. Gel fraction

The degree of crosslinking can be obtained by measuring the gel fraction through the use of the network polymer that is not soluble in any solvent. This insoluble fraction is a three dimensional network that consists of a chemical bonding of the polymer. PEGDMA 200 can be added in the acrylic resin to form crosslinking. Figure 2-8 shows the change in the degree of crosslinking according to the UV dose and to the initiator content. Here, the degree of crosslinking does not form for more than about 80% because 20% of the linear polymer formed when the prepolymer had been prepared. Figure 2-8a indicates the crosslinking formation without UV dose. In a similar manner to that in Figure 2-7a, crosslinking did not form when heating was treated for 10 min. Figures 2-8b-d indicate the change in the gel fraction with UV doses of 400, 800 and 1600 mJ/cm². The gel fraction gradually decreases, which is different from what is shown in Figure 2-7. In addition, the network structure formed with UV curing had been polymerized until 70% of the monomer was reacted, as shown in the similar gel fraction at 800 mJ/cm² and at 1600 mJ/cm² for the 0 min heating time, as compared to that shown in Figures 2-7c and 2-7d. However, for the 800 mJ/cm² UV irradiation condition, the gel fraction increased after heating due to the residual monomers contributing to the formation of the crosslinking as dual curing had proceeded through.



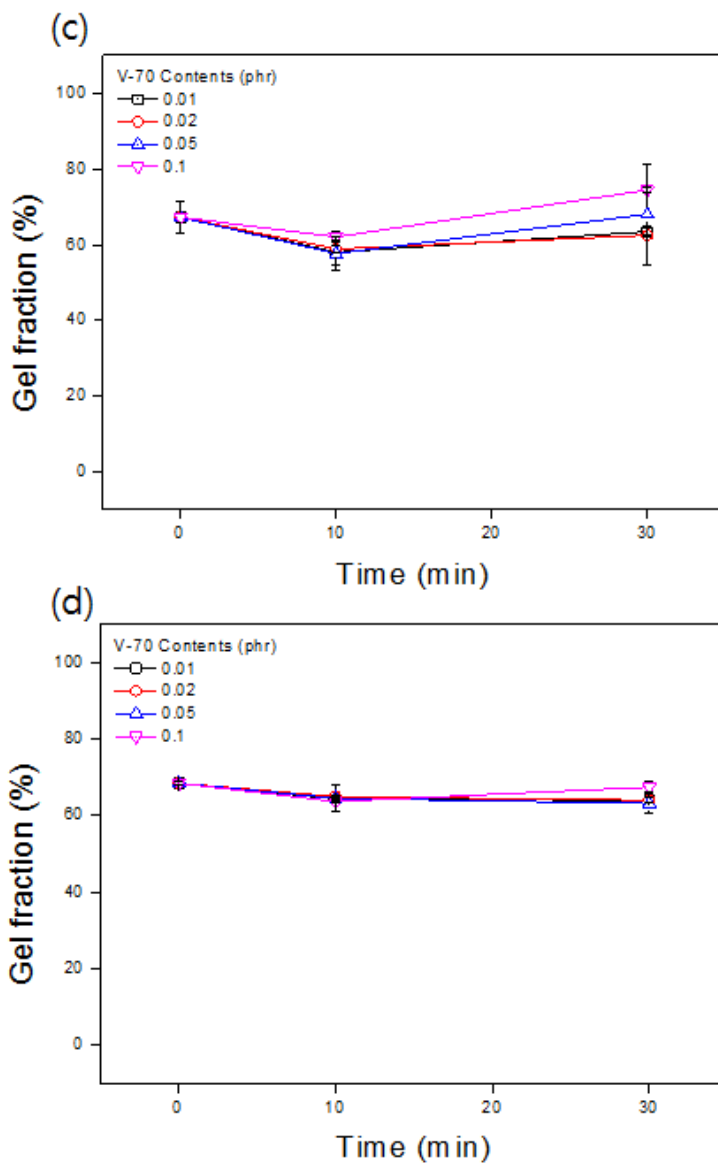


Figure 2-8. Gel fraction of the dual cured adhesives with TRI content (a) without a UV dose, and with UV doses of (b) 400 mJ/cm², (c) 800 mJ/cm² and (d) 1600 mJ/cm².

3.4. Thermal analysis of dual curable adhesives determined by DSC and TGA

Figure 2-9 shows the DSC curves of the dual curable adhesives that were used to evaluate the change in the glass transition temperature (T_g) in response to changes in the concentration of the initiator and UV dose. DCA-0400 did not exhibit a T_g in the samples exposed to a UV dose of 400 mJ/cm^2 , and it was -38.1°C for DCA-0402 and -35.4°C for DCA-0410. DCA-1600, DCA-1602 and DCA-1610 received a UV dose of 1600 mJ/cm^2 , and exhibited T_g of -32.1°C , -29.0°C and -28.7°C . The change in T_g indicates a change in the structure of the polymer because the copolymer of the resin has the same monomer composition. The increase in T_g with an increase in initiator content is mainly affected by the conversion, as shown in Figure 2-7. Since this process does not fully cure the samples with low initiator content, a low T_g is exhibited due to the formation of a low molecular weight polymer and the remaining residual monomers. With 1600 mJ/cm^2 of UV irradiation, a higher T_g was exhibited than for DCA-0410 due to the increase resulting from the formation of a higher molecular weight polymer. The 20% of conversion with UV dose of 400 mJ/cm^2 will have a lower molecular weight than when continuing the propagation due to UV curing because this is terminated during the propagation reaction. Therefore, even though it has a higher degree of crosslinking, as shown in Figure 2-8, T_g is exhibited for the high temperature. Thermal curing after 1600 mJ/cm^2 of UV irradiation increases T_g due to a decrease in the segmental mobility of the polymer. However, it was not significantly affected by the TRI content because a small amount of TRI can sufficiently react with the remaining monomers.

The TG and DTG curves are shown in Figure 2-10a and Figure 2-10b. This information is insufficient to conclude the type of the material of the samples, but information of the composition of the polymer and the thermal stability can be obtainable (Bruce Prime, 1981 and Trovati, Sanches *et al.*, 2010). The thermal stability of the network polymer is affected by the structure of the

polymer, composition and flexibility (Chattopadhyay, Panda *et al.*, 2005). The degradation in the dual curable adhesive can be divided into two steps. A weight loss occurs from 50 to 180°C and degradation is apparent from 270 to 350°C. The tendency for degradation was observed in to be similar to that of all dual curable adhesives because these have the same composition. The first step of the degradation between 50 and 180°C resulted from the volatilization of the unreacted monomer and the moisture in the adhesive film. As shown in Table 2-3, the TGA curves of the dual curable adhesives irradiated with UV dose of 400 mJ/cm² showed that the sample without added TRI exhibited a 48.4% weight loss between 50 and 200°C, and the degradation decreased by 14.6% and 5.5% with an increase in the initiator to 0.02phr and 0.1phr of TRI content. However, the dual cured adhesives irradiated with UV dose of 1600 mJ/cm² did not exhibit a significant weight loss because most of the monomer reacted with the UV light. The DTG curves show a slight increase in the thermal resistance during the second step of degradation, in a similar manner to T_g with an increase in Figure 2-9, as the TRI content and the UV irradiation increased, which is due to the decrease in the chain mobility resulting from the reaction of the remaining monomer.

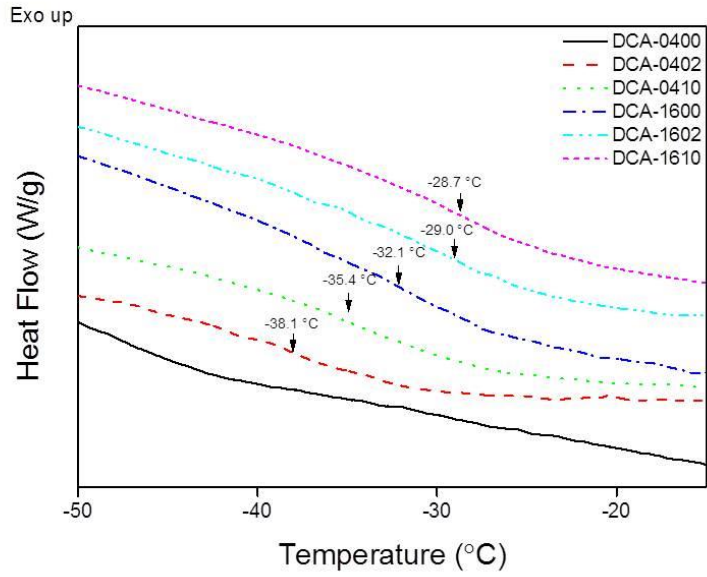


Figure 2-9. Glass transition temperature of the dual cured adhesives measured via DSC after dual curing.

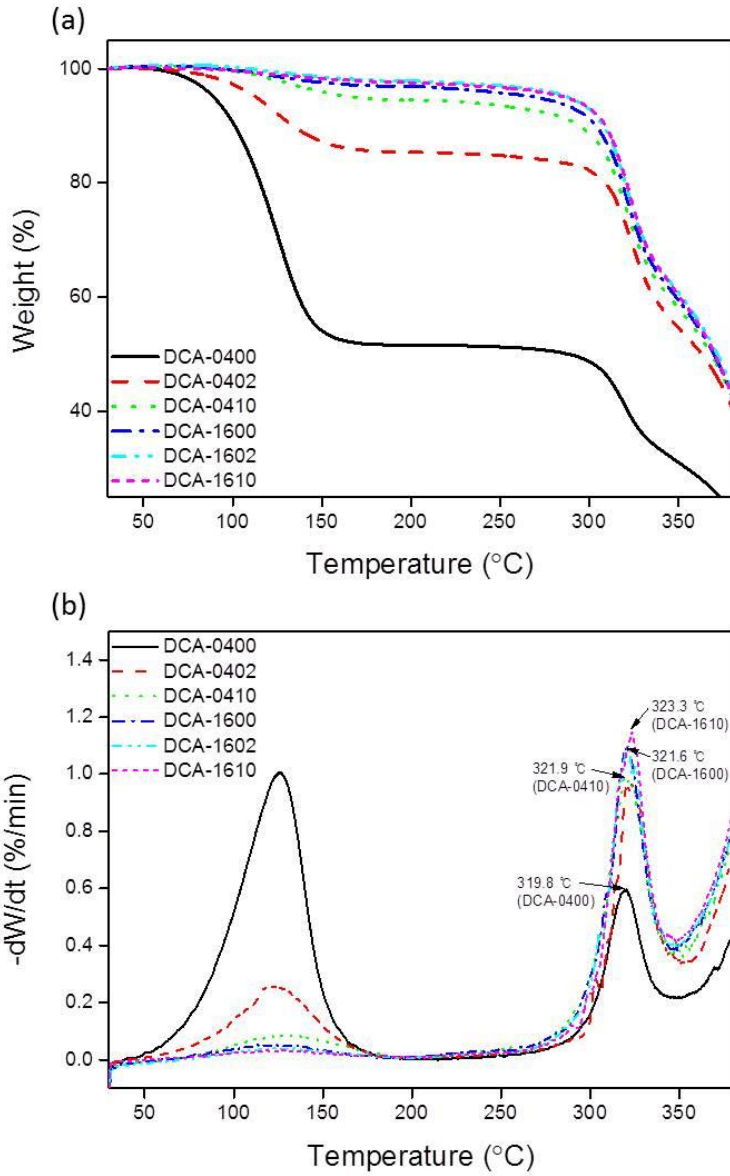


Figure 2-10. (a) TG and (b) DTG curves of the dual cured adhesives.

Table 2-3. (a) Thermal decomposition and (b) peak temperature the of DTG curves.

Samples	First step		Second step	
	Weight loss @ 200 °C (%)	Peak temperature (°C)	Weight loss @ 350 °C (%)	Peak temperature (°C)
DCA-0400	48.4	125.8	68.9	319.8
DCA-0410	5.5	129.4	42.0	321.9
DCA-1600	3.1	125.9	40.5	321.6
DCA-1610	2.5	126.3	39.6	323.3

3.5. Adhesion performance measured by peel strength, probe tack and pull-off test

The peel strength is a common method to measure the adhesion performance of pressure sensitive adhesives, and the probe tack indicates the adhesive force over a short time. The pull-off test is an important measurement for application in the display bonding process. The results of the dual curing process with different initiator contents and UV doses were assessed with respect to the peel strength, probe tack and pull-off test. Figure 2-11 shows the 180° peel strength and shows the interfacial failure for all peel strength measurement. The peel strength increases with an increase in conversion as the initiator content increases. However, the dual cured adhesive with UV dose of 800 mJ/cm² has a higher peel strength than that with 1600 mJ/cm² dose because dual cured adhesives with a lower UV dose had a higher degree of crosslinking (Bae, Lim *et al.*, 2013). In the case with UV dose of 1600 mJ/cm², the peel strength was not affected when the majority of the monomers had reacted during the UV curing process.

As shown in Figure 2-12, the probe tack increased as the UV dose and TRI contents increased. The tack of the adhesive containing 0.1phr of TRI content increased due to the linear or branched chain end that does not form a network structure, in contrast to the tendency shown for the peel strength (Czech, 2007). Dual cured adhesives with different TRI contents were affected by the increase in conversion. As shown in Figure 2-13, the pull-off strength increases with an increase in the UV dose and in the TRI content. This is influenced by the chain mobility of the polymer more than by the impact of the degree of crosslinking. In Figures 2-14a-c, the s-s curves of the dual curable adhesives are shown. As initiator was added in the samples with 400 mJ/cm² UV dose, the force and elongation increased due to the increase in conversion. The elongation and pull-off strength with UV dose of 800 mJ/cm² increased due to the formation of a semi-IPN structure with a linear polymer generated due to UV curing. However, with 1600 mJ/cm² UV dose, the DCA-

16 series shows similar adhesion strength and Young's modulus in the s-s curve due to the formation of a high molecular weight linear polymer, and little impact of the thermal curing. However, the elongation decreased along with the molecular mobility of the polymer because temporary physical bonding was formed by thermally curing the remaining monomers.

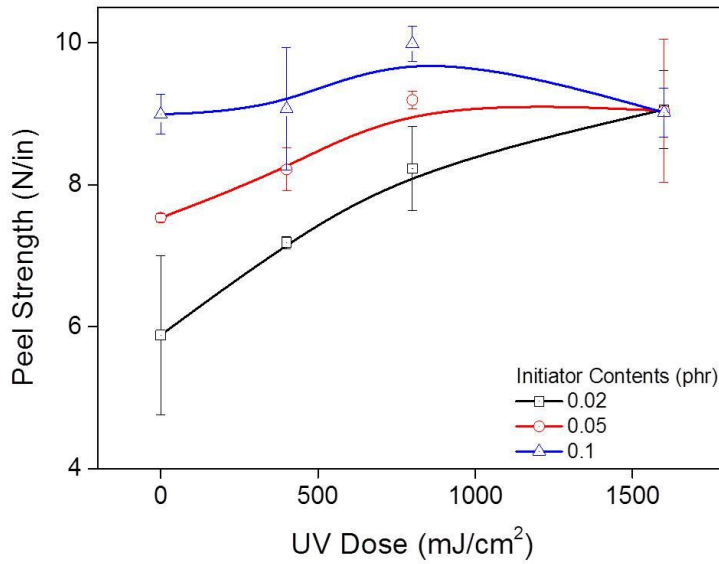


Figure 2-11. Peel strength of the dual cured adhesives with respect to the differences in UV dose and TRI content.

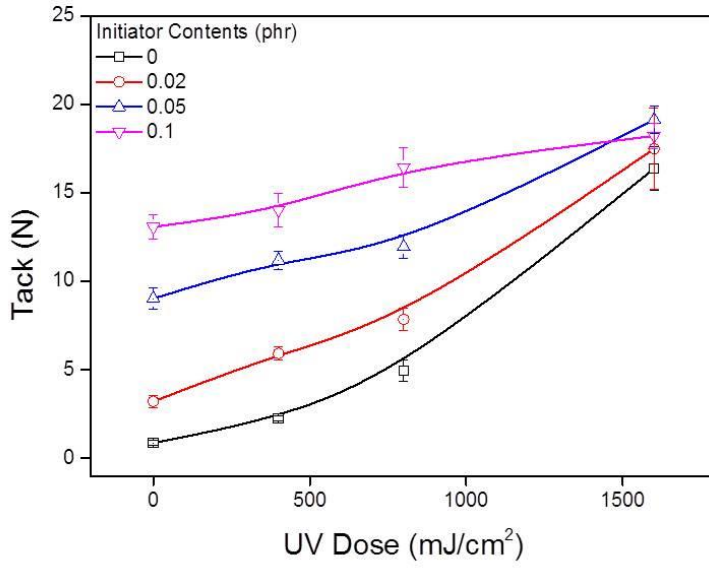


Figure 2-12. Probe tack of the dual cured adhesives with respect to the differences in the UV dose and TRI content.

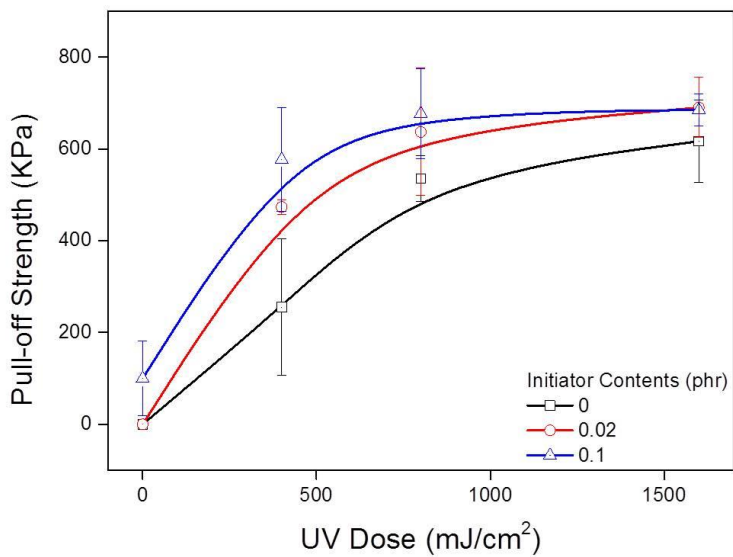
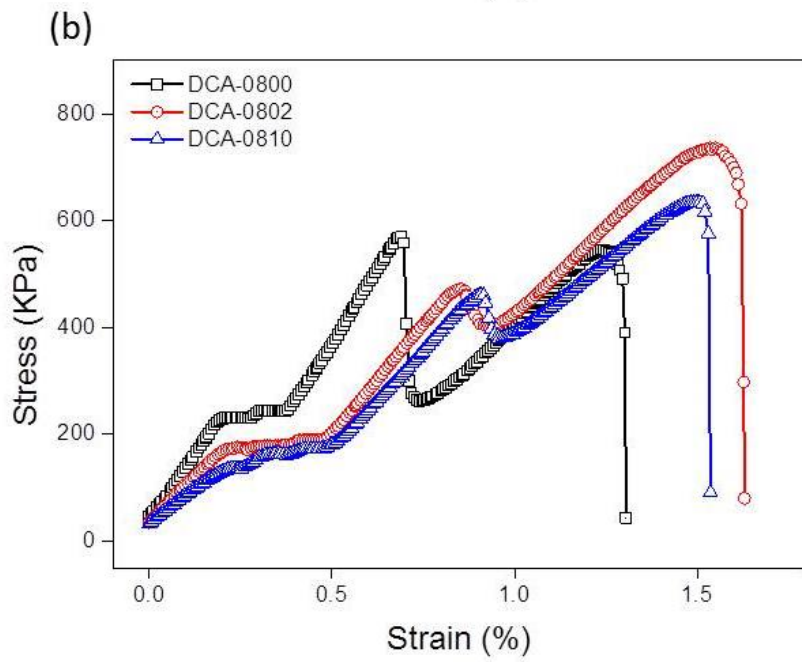
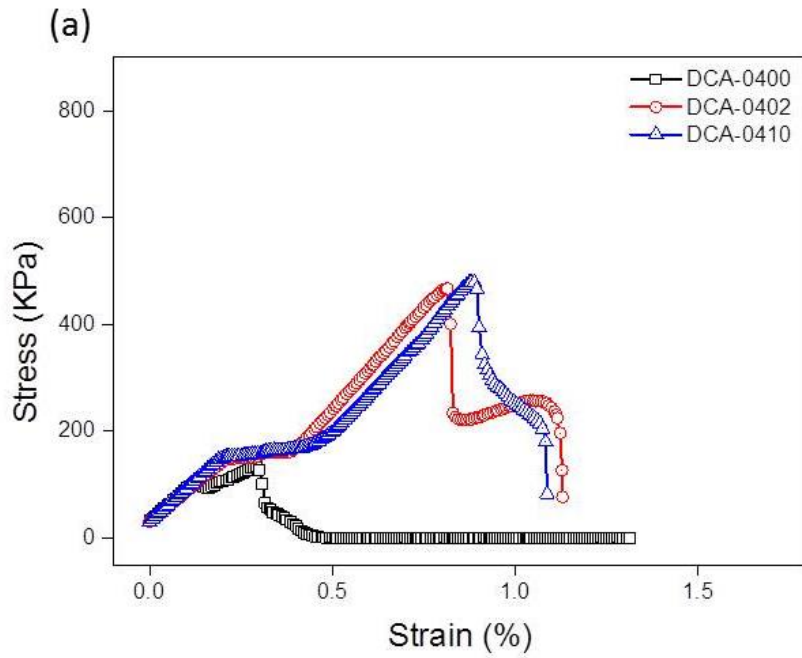


Figure 2-13. Pull-off strength of the dual cured adhesives with respect to the differences in the UV dose and TRI content.



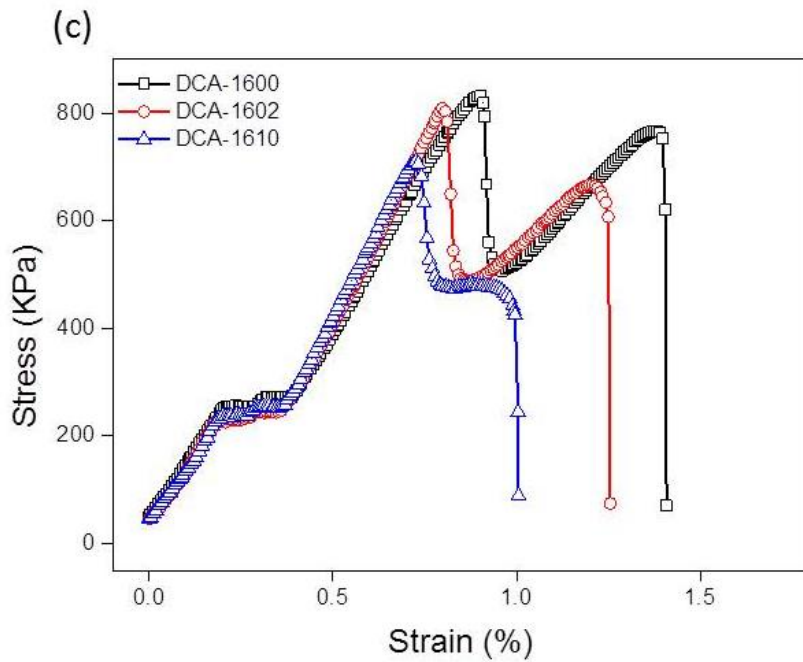


Figure 2-14. Stress-strain curves of the pull-off test for the dual cured adhesives with UV doses of (a) 400 mJ/cm², (b) 800 mJ/cm² and (c) 1600 mJ/cm².

3.6. Network formation of dual curable adhesives

We have analyzed the curing behavior, crosslinking formation, thermal properties and adhesion performance of the dual curable adhesives. As shown in Figure 2-15, all data were plotted to analyze the molecular formation of the adhesive that had been administered the dual curing process. The conversion represents the consumption of the C=C bond, the gel fraction for the formation of crosslinking, and the results in 200°C of TG show that the weight of the remaining monomer and the moisture had been removed. The conversion in Figure 2-15 is different from that shown in the data in Figure 2-8, which evaluated the curing behavior in the state resin to compare the status of the monomer at 810cm^{-1} in order to predict the overall molecular formation. The conversion and TG weight increase in a similar manner. However, the gel fraction increases steeply at the DCA-04 series and shows almost no change in the DCA-16 series. The dual cured adhesives with 400 mJ/cm^2 of UV irradiation exhibited a gel fraction that increased by only 20% with a 28.8% increase in conversion. Similarly, the gel fraction increased more sharply than conversion for DCA-0400 and DCA-1600. The gel fraction increased by 47.7% as the conversion increased by 55.6%. However, the dual cured adhesives cured with heat show a higher gel fraction than conversion.

The unreacted crosslinking agent in the polymer chain and the polymer terminated in the middle of the reaction as a result of the two curing methods of radical polymerization that were used in UV-thermal dual curing. For UV curing, the reaction terminates within 1 min because the reaction rate is very fast at room temperature. In addition, since UV curing has a high initiator content, linear polymer formation and network formation happened at the same time. In the case of the formation of the network polymer only with a multifunctional monomer, the volume relaxation was observed to have been delayed as UV curing progressed, and a high degree of crosslinking was obtained (Bowman and Peppas, 1991). However, this explanation is not adequate for the case of the semi-IPN, which contains a low level of

multifunctional monomer. In the conditions with a high level of UV irradiation, the formation of the network structure was limited because the molecular bulk mobility was restricted, and the diffusion-limited termination mechanism was dominant (Anseth, Decker *et al.*, 1995). However, thermal curing occurred at a higher temperature than UV curing, and the free volume increased. In addition, the lower TRI content than photo-initiator affected the network formation. As a result, the dual curing process provides higher network formation because the step-by-step UV-thermal curing prevents autoacceleration and mobility for the polymer. Therefore, the network is formed by linking the branch of crosslinking agent of each with the molecule to increase segmental mobility, and these characteristics can be observed in terms of the mechanical properties. With UV dose of 1600 mJ/cm², a strong tack was caused by the increase in branched chain ends, and these even obtained a high molecular weight. Furthermore, the pull-off strength increases in proportion to T_g. When the initiator is added, a small amount of monomer remaining in the dual cured adhesives reacts to form a temporary physical crosslink that increases T_g due to the decrease in the molecular mobility.

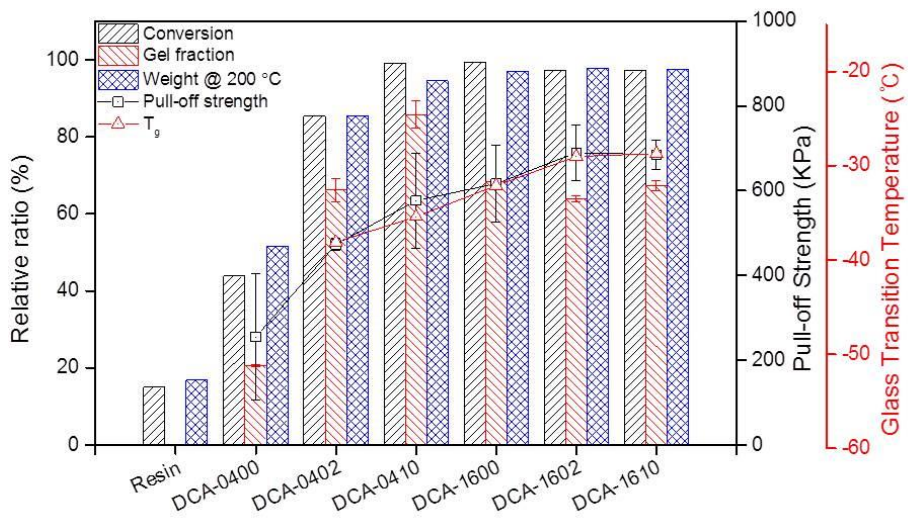


Figure 2-15. Correlation between the network formation and other properties.

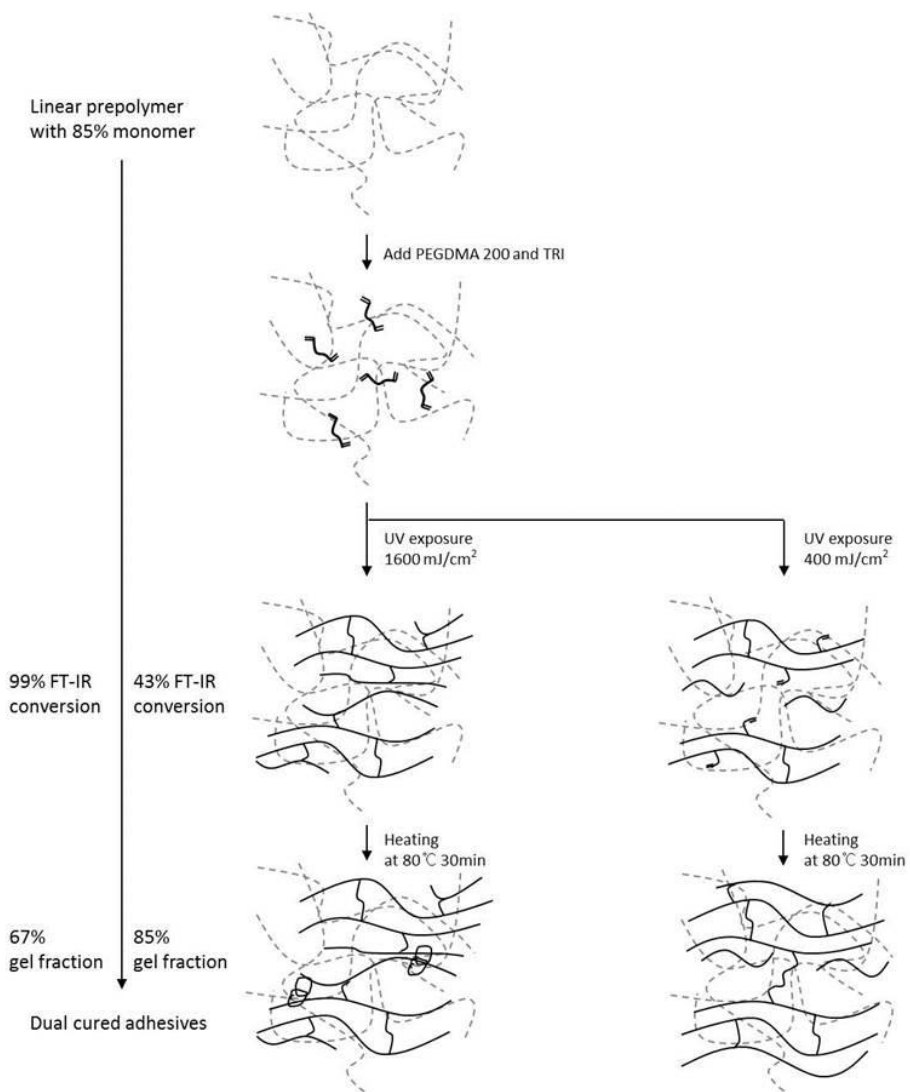


Figure 2-16. Schematic diagram of the network formation of dual curable adhesives.

4. Conclusion

Our goal was to investigate the curing behavior and the mechanical properties of dual curable adhesives using both UV and thermal radical polymerization. A dual curable system was introduced for the display bonding process to achieve curing under the shadowed area. The UV curing behavior of the UV-thermal dual curing was not hindered by the addition of TRI. On the contrary, a higher pre-UV curing and thermal initiator content improved thermal curing. We showed that the application of a dual curing system using UV-thermal radical polymerization is useful for the display bonding process due to the requirement of a low reaction temperature and a short amount of time with good adhesion performance. Relative to pure acrylic adhesives, dual curable adhesives exhibited a higher conversion rate and improved mechanical properties. Our results show that the pre-cured sample with a low UV dose formed a network structure as a result of the low initiator content and higher temperature condition that affected the formation of the gel by linking the crosslinking agent inside the chain. Despite the low molecular weight, which can adversely affect the mechanical properties, dual curable adhesives with a low UV dose had similar mechanical properties as those that received a high UV dose because they could be complemented by the network formation. In addition, the initiator content extremely affects curing and molecular forming. The 0.1phr TRI content was suitable for the dual curable system because a higher TRI content caused bubbles and yellowing, and a lower TRI content could not sufficiently cure the resin. In conclusion, the dual curable adhesives exhibit excellent adhesion for both high and low UV doses with the proper initiator content.

Chapter 3

Curing Behavior and Viscoelastic Property of Dual Curable Adhesives

1. Introduction

Because UV curing has distinct advantages, it is widely used in various industries such as ink, coating and adhesives. The recent expand of this technology is due to the advantages of the curing rate (Davison, 1999). In addition, UV curing is a solvent-free process, can be done at ambient temperature, and has a high polymerization rate (Decker *et al.*, 2001). UV radical polymerization has mainly been studied, because radical curing is achieved at a faster rate than the other curing methods such as ionic polymerization, step polymerization and vaporization. Acrylate-based resin is especially used in UV radical polymerization because of the high reactivity of monomers (Andrzejwska, 2001, Cho *et al.*, 2005). However, there are fatal drawbacks in the UV curing process. For example, the curing does not proceed in shadowed areas, such as on curved surfaces, because it is not possible for the light to penetrate (Schmid, 2001). This will have implications for the reliability factor, because any remaining unreacted monomer will act as a defect in the product. Such monomers can contaminate the other parts of the product, such as the cover glass of the display. For these reasons, only UV curing treatment is insufficient for the handling of display bonding processes.

The transparent adhesive resin used for display bonding is called optically clear resin (OCR). The applications of optical bonding adhesives include not only the simple bonding of touch screen panels (TSP), but also improvement of the image quality of the display by filling air gaps, while also protecting the TSP from external damage (Lee *et al.*, 2012). Adhesive materials for optical applications demand high transparency for improvement of quality, non-acidic conditions for prevention of TSP corrosion, appropriate viscoelastic properties for damping damage, and low shrinkage. The display bonding process between the TSP and cover glass is a UV curing process using OCR (Daniel, 2012). The TSP and cover glass were temporarily fixed by pre-curing for preventing overflow, and then the display was completely cured in the final

curing process. However, under the shadowed area, the monomers could not be cured due to interruption of the Black matrix (BM) area. Although side curing treatment was undertaken during or after the final curing process, it is not sufficient to cure the monomers under the BM area due to the flexible printed circuit board (FPCB), which interferes with the path of the UV light. Therefore, other curing methods undisturbed by obstacles are required for curing the shadowed area. We applied and investigated a UV-thermal dual curing process, as shown in Figure 3-1. A thermal initiator for curing at ambient temperature is required, because the TSP could be damaged by heating to temperatures above 100°C, and a short process time is required. In the process, both the thermal curing behavior and mechanical properties were affected by pre-UV curing degree caused by the penetration of UV light (Hwang *et al.*, 2013). To solve the curing problem related to UV curing, dual curing systems such as a redox system, isocyanate linkage and urethane linkage were investigated (Decker, 2003, Studer *et al.*, 2005), but it is difficult to apply these methods to the current process because of demand for additional processing steps.

In this study, 2,2'-azobis(4-methoxy-2,4-dimethyl valeronitrile), with a 10-hour half-life decomposition temperature of 30°C, was used as a thermal initiator for UV-thermal dual curing, as shown in Figure 3-2. However, this initiator is unstable with exceeds initiator content because azo-based initiators cause bubbles and yellowing (Studer *et al.*, 2005). For these reason, the thermal curing efficiency cannot be improved by adding excess initiator. Acrylate resin was made with 2-ethylhexyl acrylate, isobornyl acrylate and N-vinyl caprolactam. N-vinyl caprolactam was used as a non-acidic monomer instead of acrylic acid to control the glass transition temperature and to improve the cohesion properties. Resin was used in the form of a prepolymer composed of oligomer and monomer without solvent for adjustment of the viscosity. The curing kinetics of the dual curable acrylate resin was measured with various initiator contents and degrees of pre-UV irradiation. The dual curing behavior was analyzed by Fourier Transform Infrared Spectroscopy,

differential scanning calorimetry, UV-advanced rheological expansion system and gel-fraction. In addition, changes in the mechanical properties were determined using the lift-off test. The thermal degradation and curing behavior under heating conditions was evaluated by thermo-gravimetric analysis.

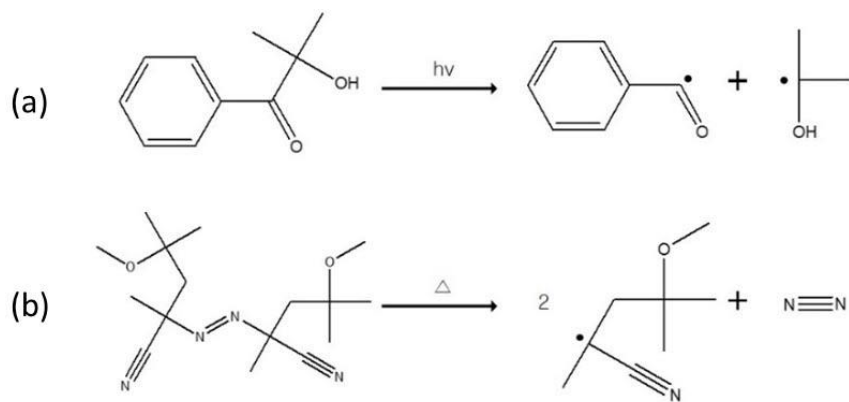


Figure 3-1. Free radical generation of (a) photo initiator and (b) thermal initiator.

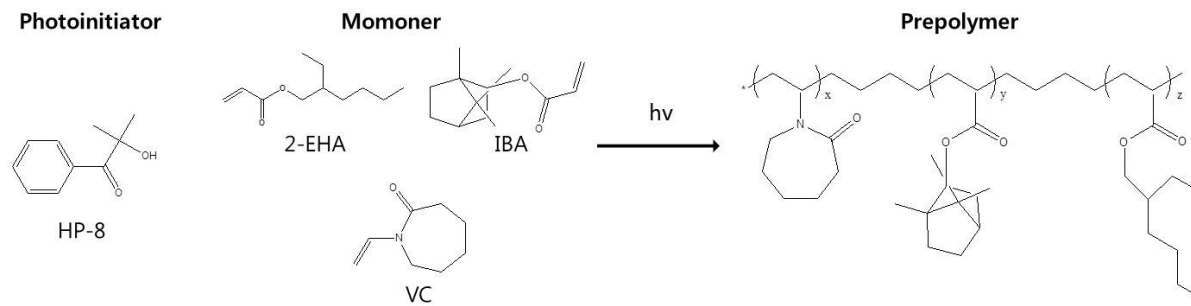


Figure 3-2. Synthesis of acrylic prepolymer.

2. Experimental

2.1. Materials

2-Ethylhexyl acrylate (2-EHA, Sigma Aldrich, USA), isobornyl acrylate (IBA, Sigma Aldrich, USA) and N-vinyl caprolactam (VC, Tokyo Chemical Industry, Japan) were used as monomers without purification. Poly(ethylene glycol (200) dimethacrylate) (PEGDMA 200, Miwon Specialty Chemical, Republic of Korea) was used as a crosslinking agent, as shown in Table 3-1. Hydroxydimethyl acetophenone (Micure HP-8, Miwon Specialty Chemical, Republic of Korea) was used as a photo initiator. 2,2'-Azobis(4-methoxy-2,4-dimethyl valeronitrile) (V-70, Wako Pure Chemical Industries, Japan) was used as a thermal initiator.

Table 3-1. Raw materials for synthesis and preparation of optically clear resin.

Function	Materials	Abbreviation	Molecular weight (g/mol)	Glass transition temperature (°C)	Contents (wt.%)	Supplier
Acrylic monomer	2-Ethylhexyl acrylate	2-EHA	184.28	-70	61	Sigma Aldrich
Acrylic monomer	Isobornyl acrylate	IBA	208.3	94	35	Sigma Aldrich
Functional monomer	N-vinyl caprolactam	VC	139.19	184	4	Tokyo Chemical Industry
Crosslinking agent	Poly(ethylene glycol (200) dimethacrylate)	PEGDMA 200	330.4	-	1phr	Miwon Specialty Chemical

2.2. Characterization methods

2.2.1. Synthesis of prepolymer

The adhesives were synthesized using 2-EHA, IBA and VC via bulk radical polymerization. Mixtures of monomers were initiated with 1wt.% Micure HP-8. Polymerization was performed in a 500 ml four-necked rounded-bottomed flask equipped with a mechanical stirrer, N₂ inlet, thermometer and LED UV lamp. The temperature was maintained at room temperature with constant stirring at 100 rpm. After N₂ purging for 30 min under constant stirring, monomer mixtures were subsequently exposed to a UV lamp (20 mW/cm²) for 70 sec at room temperature under N₂ purging (Kim *et al.*, 2013).

2.2.2. Preparation of adhesive film

UV-curable adhesive syrups were prepared by blending of the prepolymer with crosslinking agent (PEGDMA 200, 1phr) and thermal initiator. The mixture was blended by paste mixer with revolution at 600 rpm, and rotation at 500 rpm for 3 min. The syrup was coated at a thickness of 45 μm on corona-treated polyethylene terephthalate films (PET, SKC Co. LTD., Republic of Korea). The coated resin was cured by passing under a conveyor type UV-curing machine equipped with medium pressure mercury UV-lamps (154 mW/cm², main wave length: 365 nm). The irradiated UV-doses were 200, 400, 600, 800, 1600 and 2500 mJ/cm². The UV doses were measured using a UV radiometer (IL 390C Light Bug, International Light Inc.). Each adhesive, with various degrees of curing, was cured in an oven at 80°C for 60 min.

2.2.3. Fourier transform infrared (FTIR) spectroscopy

The infrared reflectance spectra were measured via the Fourier-transform infrared (FTIR) spectrometer JASCO FTIR-6100, which was employed with a Mylar beam splitter. Spectra were collected for 32 scans at a resolution of 4 cm^{-1} between 400 and 4000 cm^{-1} . Acrylate double bond conversion after a given irradiation time (t) was calculated using following equation:

$$\text{Conversion (\%)} = \frac{(A_{810})_0 / (A_{1720})_0 - (A_{810})_t / (A_{1720})_t}{(A_{810})_0 / (A_{1720})_0} \times 100$$

where, $(A_{810})_0$ is the intensity of 810 cm^{-1} at initial time, $(A_{810})_{t0}$ is the intensity of 810 cm^{-1} at time t.

2.2.4. Gel fraction

The gel fraction of the dual cured adhesives was determined by soaking the samples in toluene for 1 day at room temperature. The sample amounts are 0.2-0.3 g. In addition, the insoluble part of the adhesives was removed by filtration and dried at 70°C to a constant weight as shown in Figure 3-3. The gel fraction is calculated by the following equation:

$$\text{Gel fraction (\%)} = (W_1 / W_0) \times 100$$

where, W_0 is the weight before filtration and W_1 is the weight after filtration.

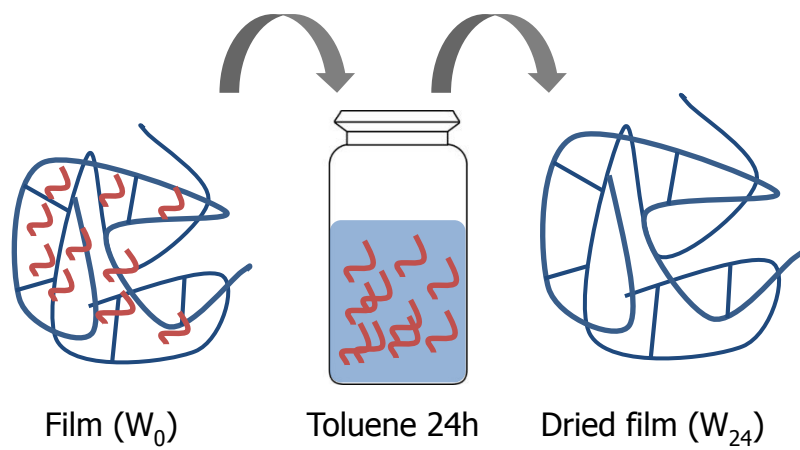


Figure 3-3. Schematic diagram of gel fraction.

2.2.5. Thermogravimetric analysis (TGA)

TGA measurement was carried out using a thermogravimetric analyzer (TGA 4000, PerkinElmer, USA). The samples of 4-5 mg were evaluated from 30°C to 400°C at a heating rate of 5 °C/min. During testing, the green composites were placed in a high quality nitrogen atmosphere (99.5% nitrogen, 0.5% oxygen content) to prevent unwanted oxidation.

2.2.6. Differential scanning calorimetry (DSC)

Differential scanning calorimetry (DSC) measurements were carried out on a TA Q200 differential scanning calorimeter with a scanning temperature range from -50 to 200°C at the scanning rate of 5 °C/min. Sample analysis was carried out on 7-8 mg. Each sample was scanned as the dynamic mode was cooled at the same rate under a nitrogen atmosphere. Thermal curing behavior was determined from the first scan. Glass transition temperature (T_g), was determined from the second scan.

2.2.7. UV-Advanced rheometric expansion system (UV-ARES) analysis

The viscoelastic properties of the acrylic adhesives were determined using an advanced rheometric expansion system (ARES, Rheometric Scientific, UK) equipped with an 8 mm parallel plate mode. The typical temperature scan range was from -30 to 150°C, at the heating rate of 2 °C/min. The cooling rate was 10 °C/min. The frequency was 1 Hz, and the gap between plates was 1 mm. In addition, the $\tan \delta$ curves from the temperature sweep tests suggested the glass transition temperature (T_g) at the second cycle. The UV light irradiation was performed using a medium-pressure mercury lamp at the intensity of 200 mW/cm² for 5-15 sec.

3. Results & Discussion

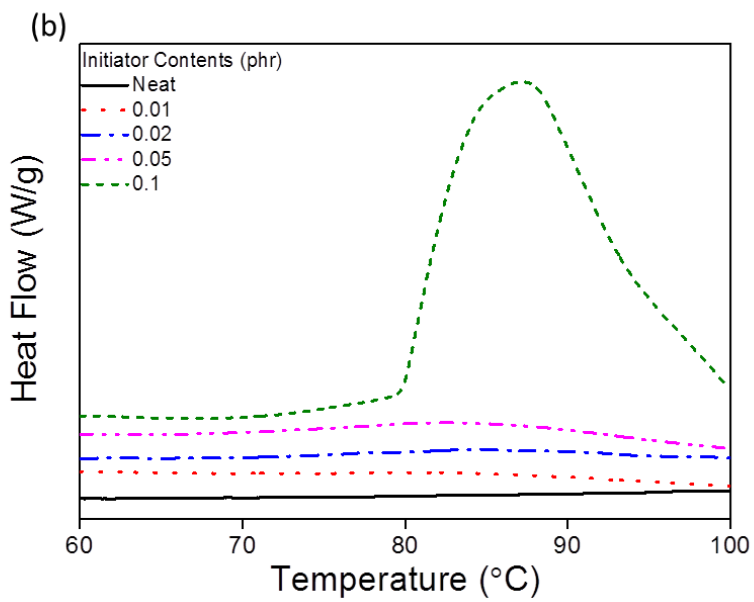
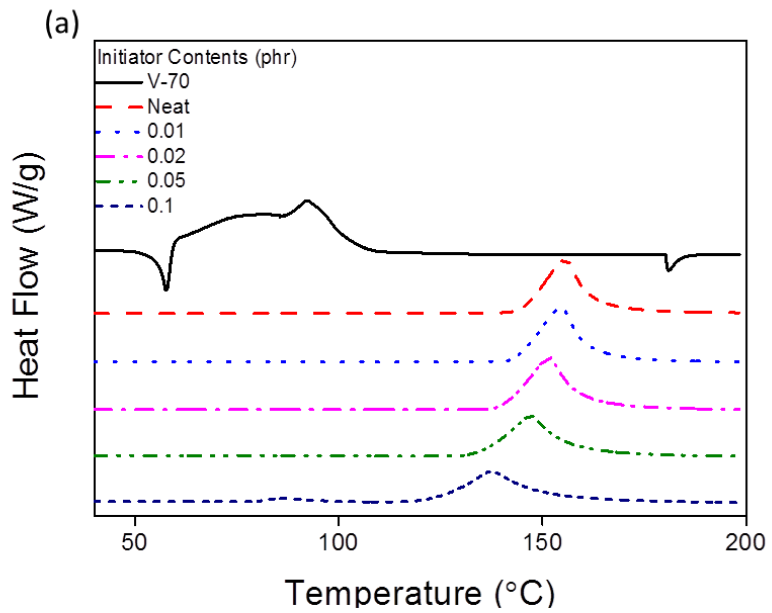
3.1. Curing behavior of acrylic adhesives determined by DSC and TGA

DSC experiments were carried out to measure the thermal curing behavior of pre-cured acrylic resin. Although the thermal initiator had a 10 hour half-life decomposition temperature of 30°C, the specific temperature should be satisfied for application to manufacture for reducing the process time. The C=C double bond is broken by radical polymerization as the temperature of acrylic resin rises and thermal initiator reacts (Bruce Prime, 1981). The exothermic reaction caused by polymerization was compared to the reaction of the thermal initiator. In the DSC curves, two kinds of exothermic peak were seen; one is between 70 to 100°C and the other between 120 to 200°C. The first peak indicates the reaction of thermal curing and the second peak shows reaction of acrylate monomer.

The change of the second exothermic peak indicates that the reaction of monomers was accelerated by an increase in the initiator content as shown in Figure 3-4a. In addition, the second exothermic peak was shifted to lower temperature with decreased height as the initiator content increased. Figure 3-4b shows that the first exothermic peak increased with an increase of the thermal initiator content from 0.01phr to 0.1phr. The exothermic peak for low initiator contents under 0.1phr was barely visible, but the peak height of the resin containing 0.1phr of initiator increased rapidly. The DSC results in Figure 3-4c also show that the height of the peak and the shift tendency were decreased as the initiator content increased. Otherwise, the exothermic peak was decreased with a shift to higher temperature due to suppression of thermal curing, depending on the pre-UV curing. Figure 3-4d shows the height of the second exothermic peak, which indicates that the reaction of the thermal initiator with monomers was decreased with increase of the UV dose, because

the initial UV curing suppressed the thermal curing. As the UV curing progressed the mobility of the polymer decreased because of the growth of the polymer and formation of a network structure.

TGA measured the weight loss which shows the ratio of polymers and indicates the degree of curing caused by the thermal curing. The results of the thermal curing behaviors of acrylic resin are shown in Figure 3-5. Decomposition progressed in two steps. The first step shows the volatilization of unreacted monomer and moisture in the adhesive film, and second step shows degradation of the polymer. Figure 3-5a shows the weight loss of the resin which was not irradiated by UV light from 30 to 400°C. The temperature at which a plateau occurred was moved from 170 to 90°C, as the amount of initiator increased. In addition, the weight loss was decreased from 72.6% to 5.3% at the plateau area. The weight loss of the neat resin, 72.6%, was caused by the synthesis of prepolymer. In Figure 3-5b the adhesives with 400 mJ/cm² of UV dose also shows a change with gap of weight loss decreasing. In contrast, Figure 3-5c and Figure 3-5d show the weight loss of the adhesives with various initiator contents and UV doses. In particular, the film containing 0.1phr initiator without UV treatment had greater weight loss than the adhesive with UV dose of 800 mJ/cm², because thermal curing is suppressed by pre-UV curing. The change in weight loss was decreased as the pre-UV irradiation increased. With UV doses of 800 mJ/cm² and 1600 mJ/cm², thermal curing did not affect the weight loss. Also, with 800 mJ/cm² UV dose the weight loss shows gel fraction under 80% due to the restrained thermal curing. Therefore, the TGA results indicate that the UV dose suppressed thermal curing because the radical is caged by the decreasing mobility of the polymer.



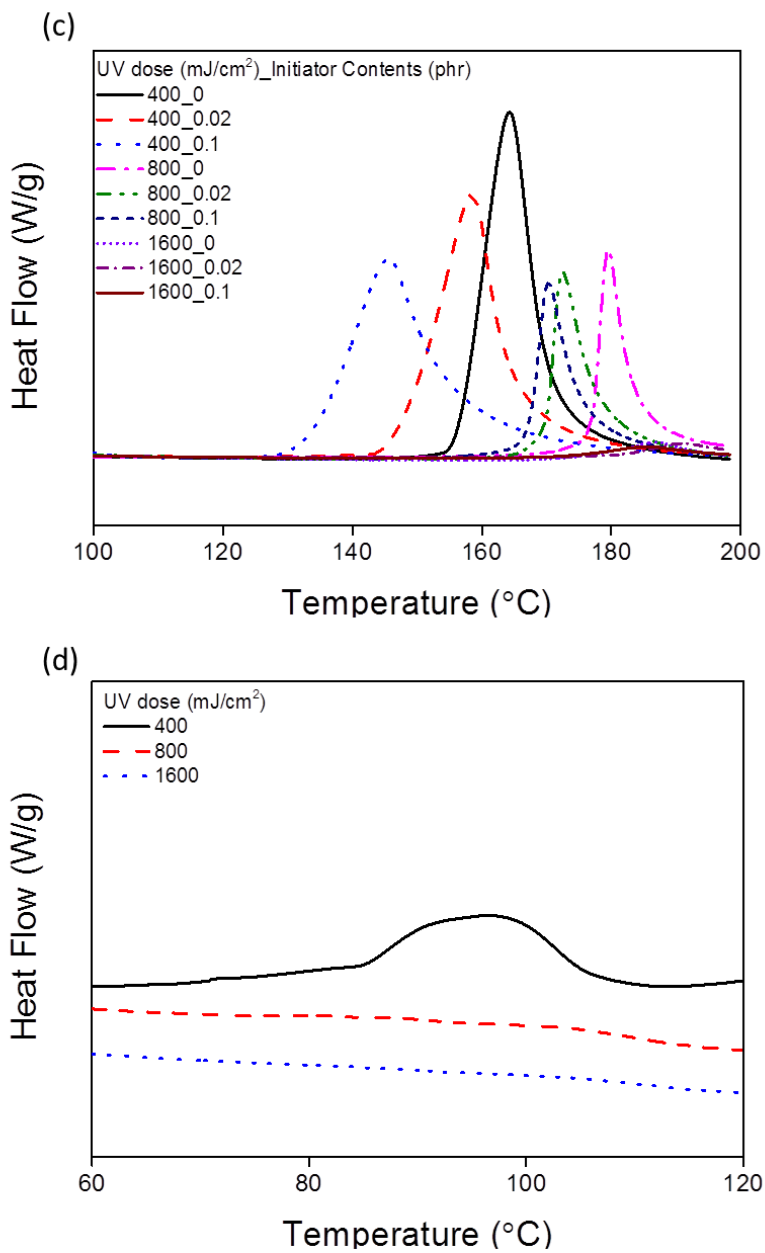
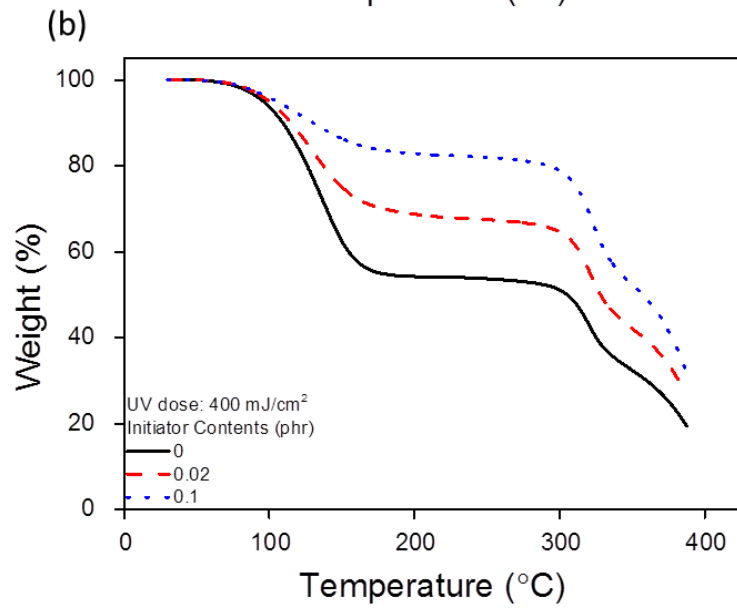
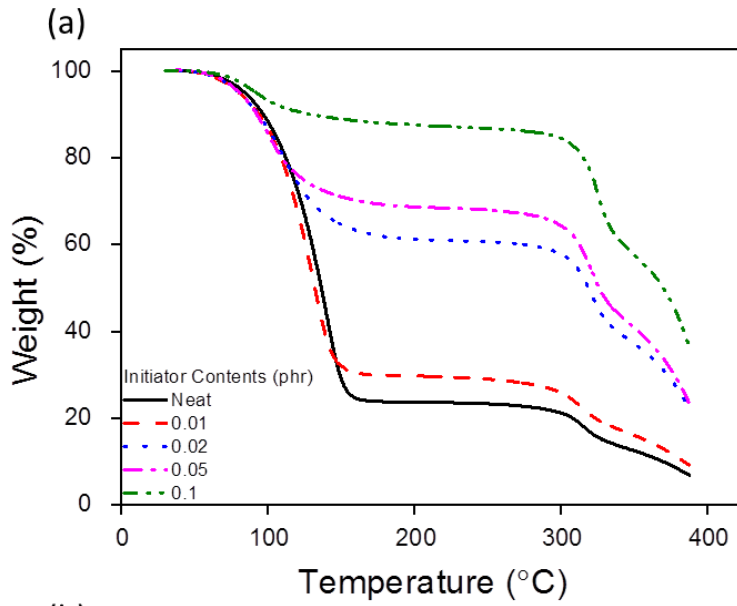


Figure 3-4. Curing behavior with different initiator contents of (a) acrylic resin, and (c) with UV doses of 400, 800 and 1600 mJ/cm². Exothermic peaks of reaction of thermal initiator (b) without UV dose and (d) with UV doses of 400, 800 and 1600 mJ/cm².



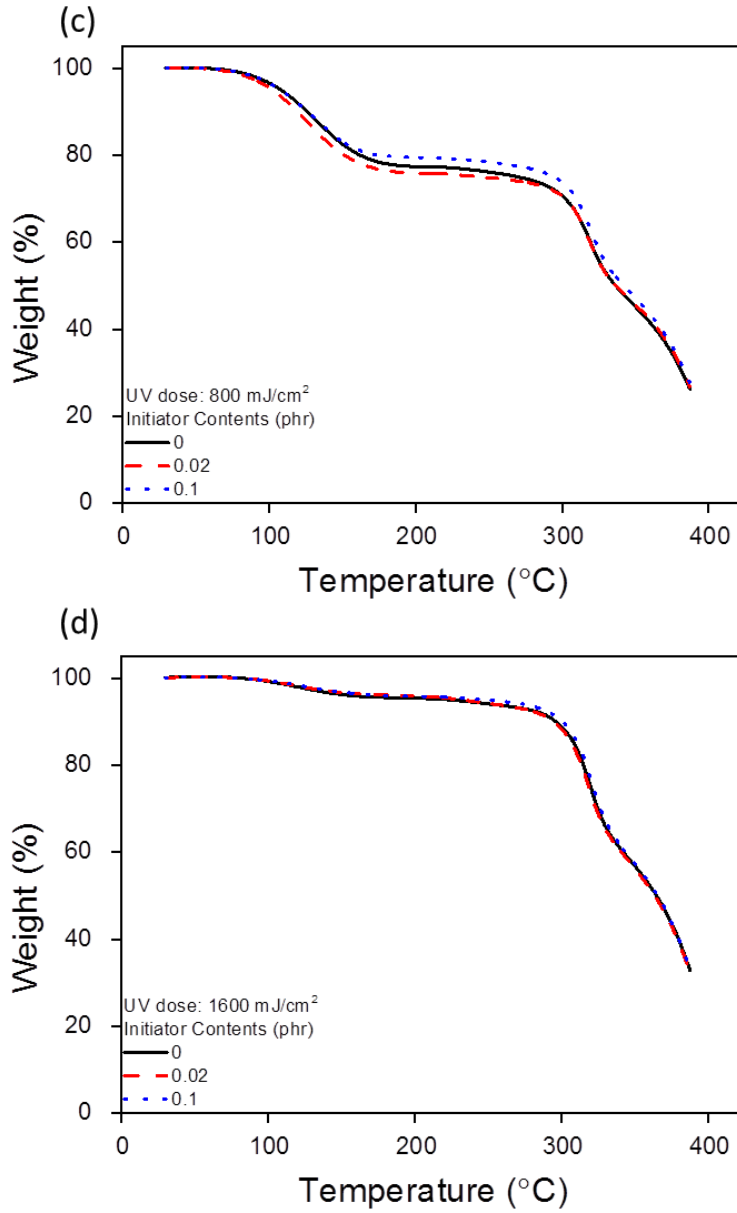


Figure 3-5. Thermogravimetric analysis with different initiator contents (a) without UV dose, and with UV doses of (b) 400 mJ/cm², (c) 800 mJ/cm² and (d) 1600 mJ/cm².

3.2. FT-IR conversion

FT-IR was measured in order to analyze the amount of C=C double bonds in the acrylic resin. C=C double bonds are broken as polymerization proceeds, and this chemical reaction can be confirmed by investigating the height of the peak at 810 cm^{-1} (Chiou *et al.*, 1997, Bai *et al.*, 2006). Figure 3-6 shows the change of conversion according to the amount of initiator and UV dose. Conversion was increased as the UV dose and the concentration of thermal initiator increased. The acrylic adhesive containing under 0.02phr of thermal initiator without UV irradiation could not be cured completely due to lack of radicals. Because 2,2'-Azobis(4-methoxy-2,4-dimethyl valeronitrile) has high reactivity, it cannot be used above 0.1phr due to its insolubility, yellowing, and bubbling. FT-IR results show that less than 0.1phr of thermal initiator could cure the whole monomers. Although initial conversion was increased with an increase of the UV dose, the adhesives were not fully cured because thermal curing efficiency is decreased by pre-UV curing. With UV dose of 400 mJ/cm^2 , the conversion was increased with addition of thermal initiator. However, conversion at 800mJ/cm^2 was lower than conversion at 400 mJ/cm^2 because the thermal curing is suppressed as UV curing proceeds.

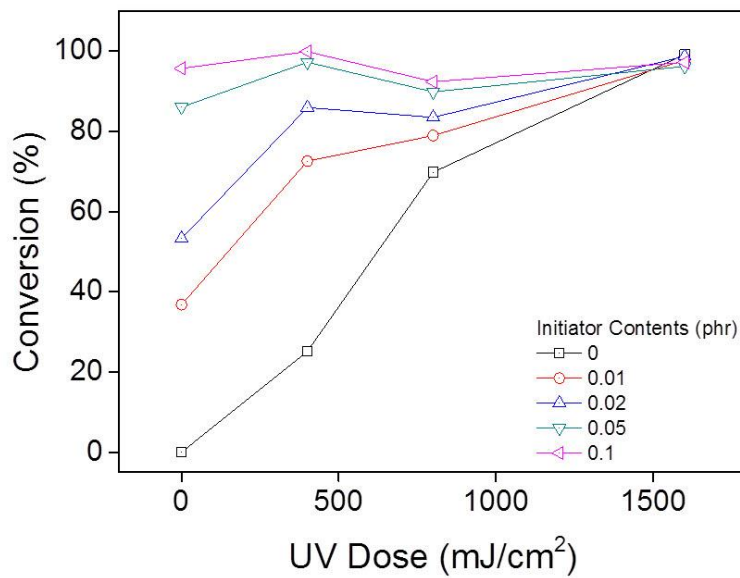


Figure 3-6. FT-IR conversion at 810 cm^{-1} after dual curing as a function of UV dose and TRI content.

3.3. Gel fraction

The gel fraction was measured to investigate the crosslinking formation of the dual curable resin. Figure 3-7 shows that the change of the gel fraction was dependent on the thermal initiator content and UV dose. The gel fraction increased with increasing initiator content, because the amount of monomer per initiator was limited. In addition, the gel fraction increased with decreasing UV dose due to the formation of a network structure. Thermal curing after UV irradiation improves formation of network structure, although UV curing cannot affect the crosslinking structure above a UV dose of 800 mJ/cm². Notably, with a 400 mJ/cm² UV dose, formation of the network is accelerated. Also, network structure was highly formed even in low concentration of thermal initiator. The gel fraction results show that improvement of thermal curing efficiency improves formation of crosslinking.

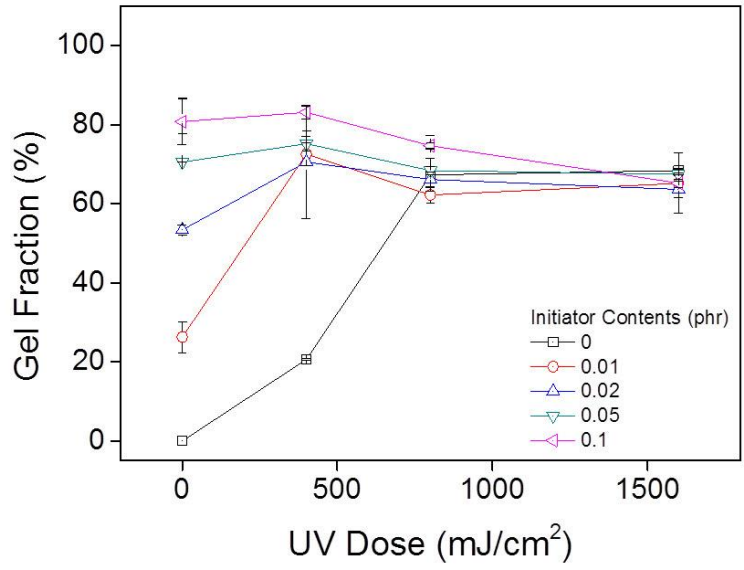


Figure 3-7. Gel fraction after dual curing as a function of UV dose and TRI content.

3.4. Curing behavior and viscoelastic properties determined by UV-ARES

UV-ARES was measured for examination of the UV-thermal dual curing behavior at various UV doses by dynamic temperature sweep. The rheological properties of dual curable resin can provide quantitative data for protecting the TSP and display and adhesion performance (Satas, 1999, Chang *et al.*, 2005). UV curing behavior, thermal curing behavior and rheological properties were measured for the same sample by controlling the curing steps. Figures 3-8a-c show the UV curing behavior of resin according to thermal initiator content. The storage modulus was not changed according to initiator content after UV curing. These results indicate that addition of thermal initiator did not influence the UV curing behavior and storage modulus. Figures 3-9a-c show the ramp test from 30 to 150°C for measurement of the thermal curing behavior depending on the initiator content and pre-UV irradiation. As thermal initiator content increased, the storage modulus was increased because of reaction of the thermal initiator. In addition, the increase of storage modulus was constrained by pre-UV curing, because polymerization decreased the mobility of the polymer. With 800 mJ/cm² and 1600 mJ/cm² UV doses, thermal curing cannot improve storage modulus. Also, reaction temperature of the thermal initiation was accelerated as concentration of thermal initiator increased.

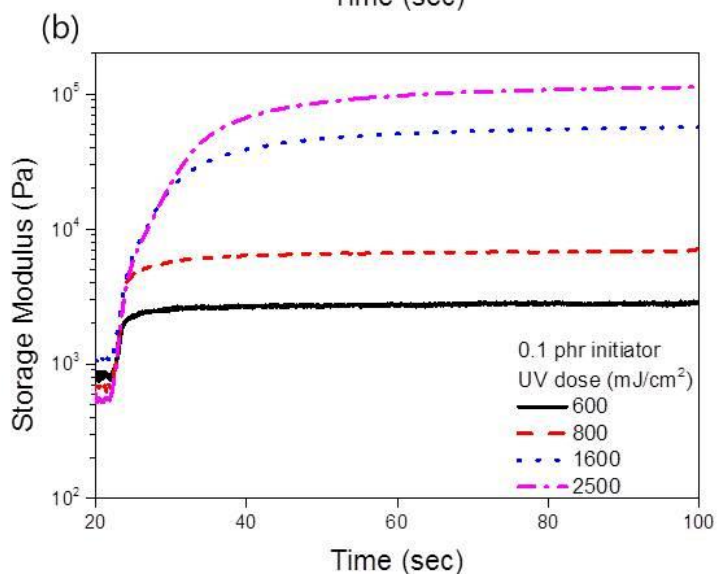
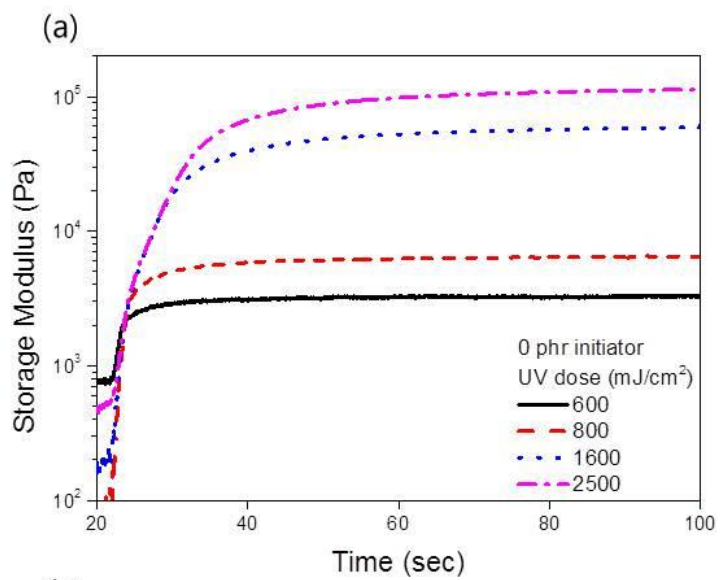
The viscoelastic properties of the dual-curable acrylic adhesive are shown in Figures 3-10a-c. The storage modulus at the plateau area was higher than that of the low UV dose adhesive due to the formation of crosslinking. Also, storage modulus at room temperature showed similar values in adhesives with 0.1phr thermal initiator. The UV-ARES results provide information for application of the process. The thermal initiator rarely affected the viscoelastic properties of the UV curable zone, while giving proper curing behavior under the shadowed area. In Figure 3-11 shows glass transition temperature with

increase of the UV dose and concentration of thermal initiator. When the UV dose was increased, the adhesive had higher T_g because of higher molecular weight of polymer. However, T_g shows higher value at 600 mJ/cm² than 800 mJ/cm² of dual cured adhesives because of higher crosslinking formation.

The results explaining the effect of dual curing on the formation of crosslinking are shown in Figure 3-12. The gel fraction per conversion was calculated by $\Delta G/\Delta C \times \text{remaining monomers}$. The average molecular weight between crosslinks, M_c , was derived from the equation below, based on rubbery elasticity (Cho, 1996). However, the crosslinking density was higher in low UV dose film because the IPN structure was formed with lower contents of thermal initiator.

$$G_N^0 = \frac{\rho RT}{M_c}$$

Where, G_N is the storage modulus, ρ is the density, R is the gas constant, T is the absolute temperature and M_c is the average molecular weight between crosslinks. M_c was calculated using the equation. This result shows that the network structure formed by thermal curing in low UV dose had higher crosslinking density. The network structure with high crosslinking density affects improvement the T_g of dual cured adhesives, which causes decrease in mobility of the polymer.



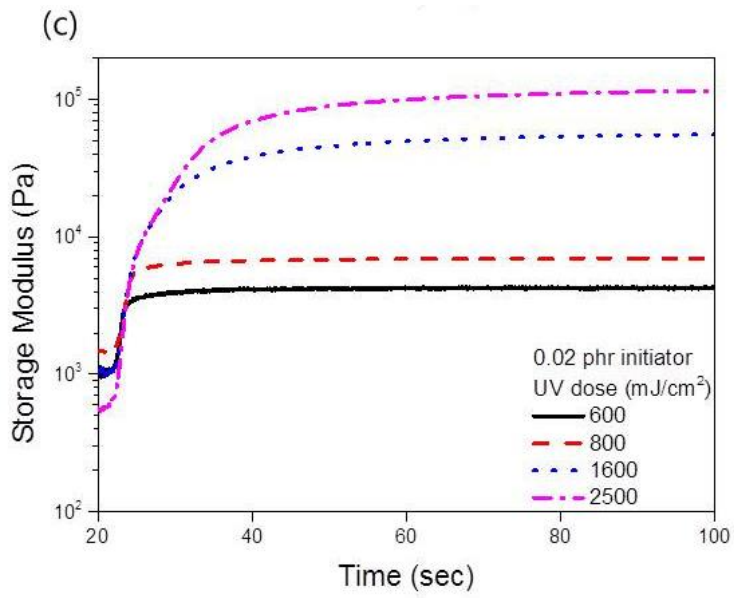
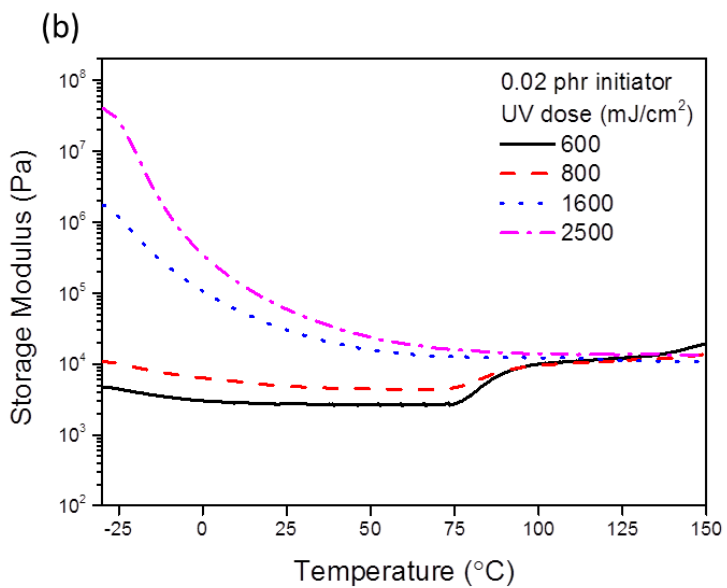
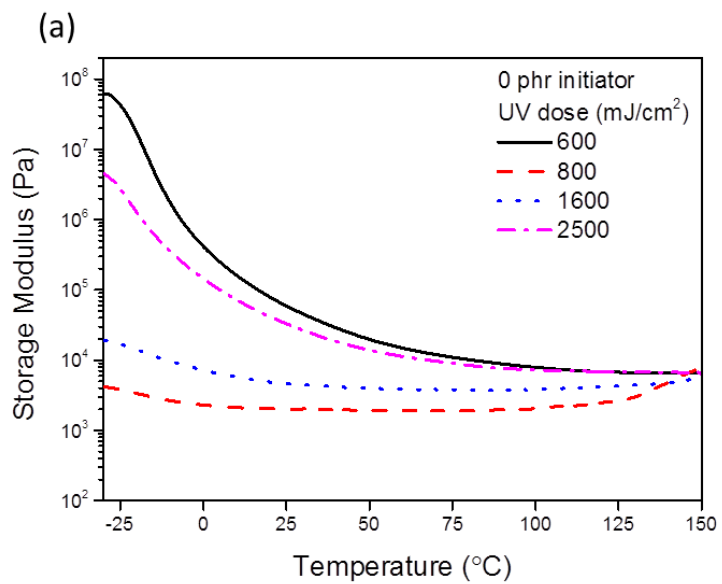


Figure 3-8. Storage modulus of dual curable resin as a function of TRI contents for (a) 0phr, (b) 0.02phr, and (c) 0.1phr with UV curing.



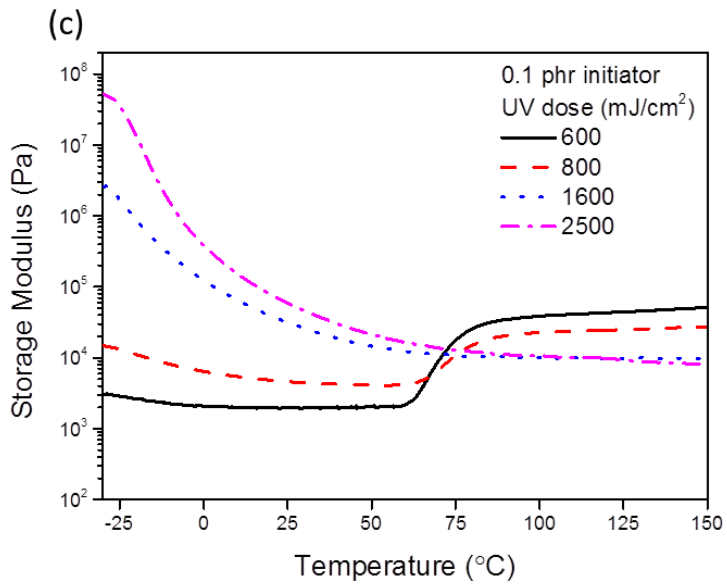
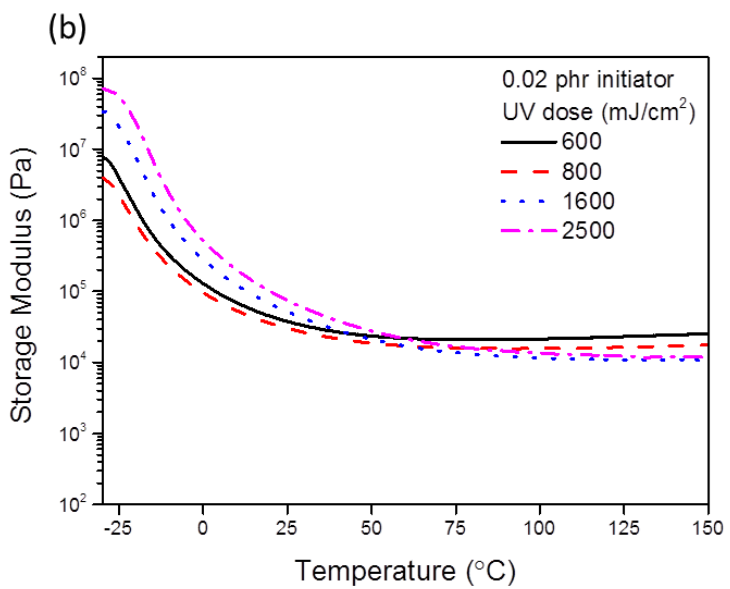
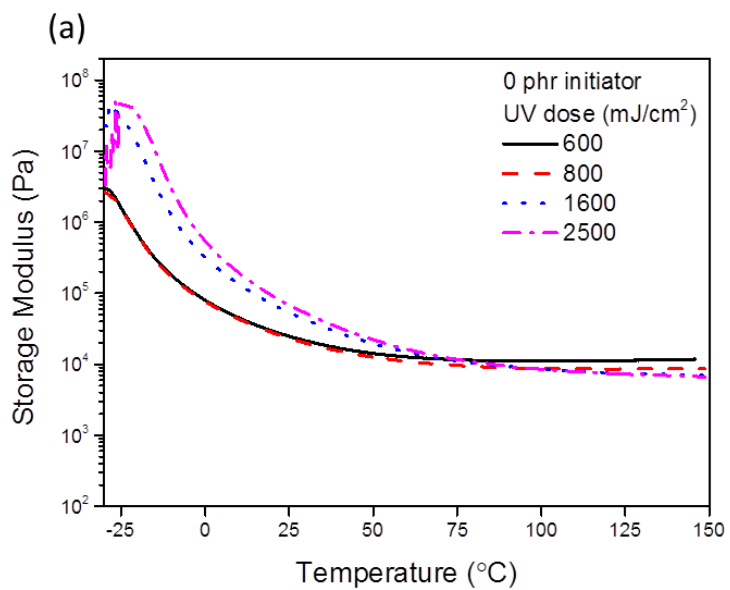


Figure 3-9. Storage modulus of dual curable resin as a function of TRI contents for (a) 0phr, (b) 0.02phr, and (c) 0.1phr for thermal curing.



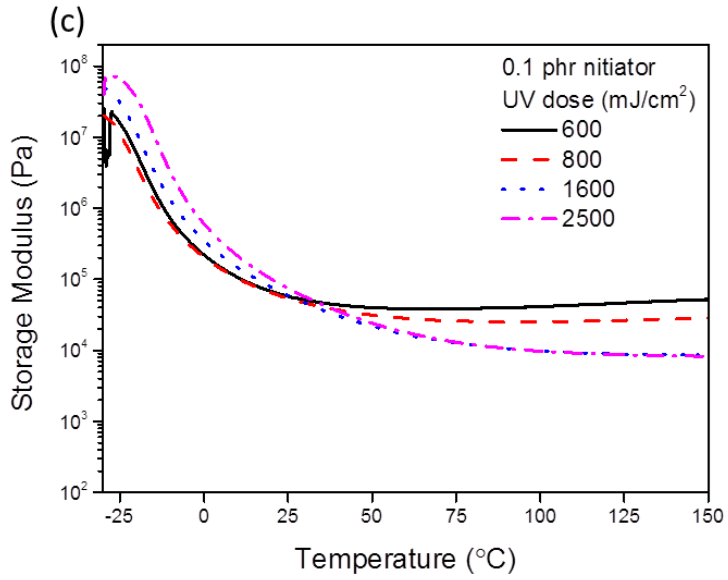


Figure 3-10. Storage modulus of dual curable resin as a function of initiator contents (a) 0phr, (b) 0.02phr and (c) 0.1phr after dual curing for measurement of the viscoelastic properties.

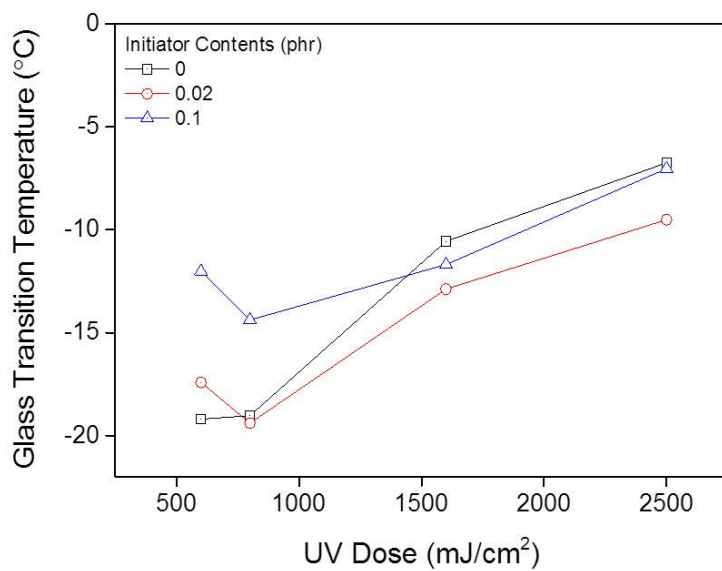


Figure 3-11. Glass transition temperature of acrylic adhesives measured by UV-ARES after dual curing.

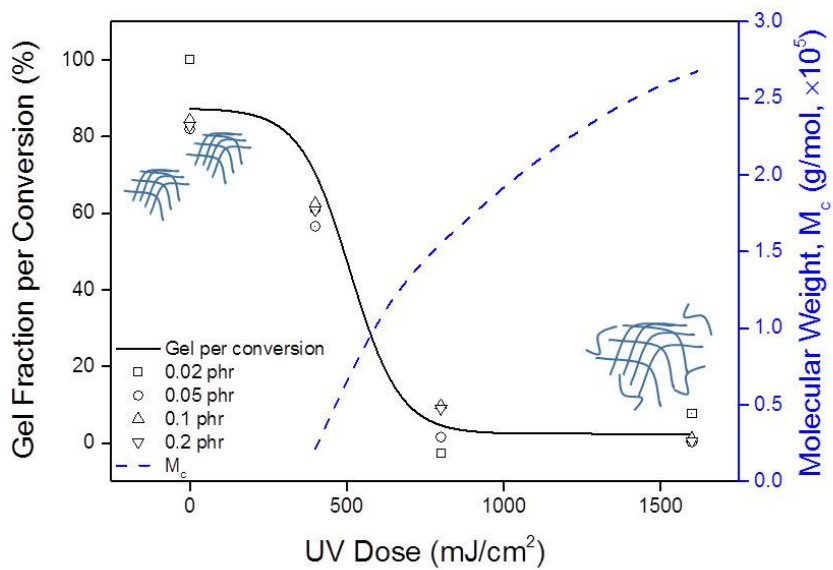


Figure 3-12. The effect of UV dose on crosslinking formation and average molecular weight between crosslinks.

4. Conclusion

We demonstrated the curing behavior and viscoelastic property of dual curable adhesives based on a radical initiation system. The curing behavior of dual curable adhesive prepared with 2,2'-azobis(4-methoxy-2,4-dimethyl valeronitrile) was investigated. The thermal initiator can improve conversion and viscoelasticity with low concentration and reaction temperature. Addition of the thermal initiator did not affect to UV curing behavior. As the thermal initiator content increased, thermal curing efficiency increased, as shown in the DSC and TGA observations. Also, thermal curing was suppressed as the UV dose increased. However, with low UV dose, thermal initiation accelerated. FT-IR results showed that concentration of the thermal initiator under 0.1phr provided thermal curing capability for dual curable adhesives. Also, the formation of network structure was increased by thermal curing with low UV dose. The glass transition temperature affected the curing behavior, which had minimum values with 800 mJ/cm² UV dose due to the formation of network structure in lower UV dose and higher molecular weight compared to higher UV dose. The storage modulus at room temperature increased with increasing initiator content. In addition, the storage modulus of the plateau area increased only with low UV dose due to the suppression of thermal curing by pre-UV curing. ARES results indicated that network structure formed by dual curing in shadowed area has higher crosslinking density.

Chapter 4

Concluding Remarks

UV-thermal dual curing system was investigated for application of display bonding process. In order to enhance the conversion under the shadow area, 2,2'-azobis(4-methoxy-2,4-dimethyl valeronitrile) was introduced to acrylic resin. Acrylic prepolymer copolymerized with 2-EHA, IBA and NVC was used as base resin. PEGDMA 200 was added to the prepolymer to form network structure. Thermal property, adhesion performance, viscoelastic property and curing behavior were investigated in accordance with thermal initiator contents and pre-UV irradiation conditions. The curing behavior was observed through FT-IR ATR, photo-DSC, UV-ARES and TGA. Network formation was investigated by gel fraction. TGA and DSC were used to measure thermal property. The peel strength, probe tack and pull-off test were used for investigating the adhesion performance.

1. Thermal property and adhesion performance of dual curable adhesives

To improve the conversion of OCR, thermal initiator with 30°C of 10 hour half-life decomposition temperature was used. The curing behavior in the state of resin was measured by photo-DSC. UV curing kinetics did not change as the thermal initiator was added. Thermal curing was accelerated as the thermal initiator contents increased. But, with low UV dose, the thermal curing promoted. FT-IR ATR shows that the chemical reaction did not change after dual curing, compared to the spectra of the only UV curing condition. C=C bond decomposition provided information about the proper contents of thermal initiator and acceleration of thermal curing with increasing UV dose. Increasing the thermal initiator contents and UV dose allowed glass transition temperature and thermal resistance to increase. When thermal initiator concentration was high, the thermal properties increased because the dual curable adhesives had high degree of crosslinking. However, high molecular weight polymer had an effect on thermal properties with high UV dose condition. For adhesion performance, the peel strength had the highest force

with 800 mJ/cm² of UV dose due to the formation of crosslinking. But the probe tack increased consistently as the conversion increased. The pull-off strength had similar tendency with the change of glass transition temperature. To conclude, thermal initiator contents of 0.1phr is the proper conditions for dual curing when using 2,2'-azobis(4-methoxy-2,4-dimethyl valeronitrile). The thermal properties and adhesion performance are mainly affected by the network formation in a low UV dose condition. By contrast, thermal initiator rarely influences the properties of dual curable adhesives with high UV dose.

2. Curing behavior and viscoelastic property of dual curable adhesives

The curing behavior and viscoelastic property of dual curable adhesives based on radical initiation system were investigated. Adding thermal initiator did not affect the UV curing behavior. But, adding thermal initiator accelerated the thermal curing efficiency. In addition, pre-UV irradiation hindered the thermal curing. Thermal initiation was accelerated only with low UV dose condition. FT-IR results show that the concentration of thermal initiator under 0.1phr can provide the thermal curing capability at dual curable adhesives. Also, the formation of network structure was increased by thermal curing in low UV dose condition. The glass transition temperature was affected by the curing behavior. T_g had minimum values at 800 mJ/cm² of UV dose. It is caused by the formation of the network structure in lower UV dose and the high molecular weight polymer in higher UV dose. The storage modulus at room temperature increased with increasing initiator content. In addition, the crosslinking density which was calculated with storage modulus at plateau area increased as UV dose decreased in dual curing process. This was caused due to the suppression of thermal curing by pre-UV curing. Therefore, dual curable adhesives under shadowed area formed network structure with higher crosslinking density and degree of crosslinking

References

Andrzejwska, E. (2001). Photopolymerization kinetics of multifunctional monomers. *Progress in Polymer Science* 26: 605-665.

Anseth, K. S. and C. N. Bowman (1995). Kinetic gelation predictions of species aggregation in tetrafunctional monomer polymerizations. *Journal of Polymer Science Part B-Polymer Physics* 33(12): 1769-1780.

Anseth, K. S., C. N. Bowman and N. A. Peppas (1993). Dynamic-mechanical studies of the glass-transition temperature of photopolymerized multifunctional acrylates. *Polymer Bulletin* 31(2): 229-233.

Anseth, K. S., C. Decker and C. N. Bowman (1995). Real-time infrared characterization of reaction-diffusion during multifunctional monomer polymerizations. *Macromolecules* 28(11): 4040-4043.

Anseth, K. S. and D. J. Quick (2001). Polymerizations of multifunctional anhydride monomers to form highly crosslinked degradable networks. *Macromolecular Rapid Communications* 22(8): 564-572.

Anseth, K. S., C. M. Wang and C. N. Bowman (1994). Reaction behavior and kinetic constants for photopolymerizations of multi(Meth)acrylate monomers. *Polymer* 35(15): 3243-3250.

Bae, K.Y., D.H. Lim, J.W. Park, H.J. Kim, H.M. Jeong and A. Takemura (2013). Adhesion performance and surface characteristics of low surface energy psas fluorinated by UV polymerization. *Polymer Engineering & Science* 53(9): 1968-1978.

Bai, C. Y., X. Y. Zhang, J. B. Dai and W. H. Li (2006). A new UV curable waterborne polyurethane: Effect of CC content on the film properties.

Progress in Organic Coatings 55(3): 291-295.

Boey, F., S. K. Rath, A. K. Ng and M. J. M. Abadie (2002). Cationic UV cure kinetics for multifunctional epoxies. *Journal of Applied Polymer Science* 86(2): 518-525.

Bowman, C. N. and N. A. Peppas (1991). Coupling of kinetics and volume relaxation during polymerizations of multiacrylates and multimethacrylates. *Macromolecules* 24(8): 1914-1920.

Bruce Prime, R. (1981). *Thermal characterisation of polymeric materials*. New York, Academic Press.

Carlborg, C. F., A. Vastesson, Y. Liu, W. van der Wijngaart, M. Johansson and T. Haraldsson (2014). Functional off-stoichiometry thiol-ene-epoxy thermosets featuring temporally controlled curing stages via an UV/UV dual cure process. *Journal of Polymer Science Part A: Polymer Chemistry* 52(18): 2604-2615.

Chang, E. P., Holguin and Daniel (2005). Curable optically clear pressure-sensitive adhesives. *The Journal of Adhesion* 81(5): 495-508.

Chattopadhyay, D. K., S. S. Panda and K. V. S. N. Raju (2005). Thermal and mechanical properties of epoxy acrylate/methacrylates UV cured coatings. *Progress in Organic Coatings* 54(1): 10-19.

Chiou, B. S. and S. A. Khan (1997). Real-time FTIR and in situ rheological studies on the UV curing kinetics of thiol-ene polymers. *Macromolecules* 30(23): 7322-7328.

Cho, J.D. and J.W. Hong (2005). Photo-curing kinetics for the UV-initiated cationic polymerization of a cycloaliphatic diepoxide system photosensitized by thioxanthone. *European Polymer Journal* 41(2): 367-374.

Cho, K. (1996). Effect of molecular weight between crosslinks on fracture behaviour of diallylterephthalate resins. *Polymer* 37(5): 813-817.

Cramer, N. B., J. p. Scott and C. N. Bowman (2002). photopolymerizations of Thiol-Ene Polymers without photoinitiators. *Macromolecules* 35: 5361-5365.

Czech, Z. (2003). Crosslinking of pressure sensitive adhesive based on water-borne acrylate. *Polymer International* 52(3): 347-357.

Czech, Z. (2007). Synthesis and cross-linking of acrylic PSA systems. *Journal of Adhesion Science and Technology* 21(7): 625-635.

Czech, Z. and A. Butwin (2009). Butyl acrylate/4-acryloyloxy benzophenone copolymers as photoreactive UV-crosslinkable pressure-sensitive adhesives. *Polish Journal of Chemical Technology* 11(3): 1-4.

Daniel, L. (2012). Liquid optically clear adhesive for display applications. proceeding of display week 2012 exhibitors' form.

Davison, S. (1999). Technology and applications of UV and EB curing. London: SITA Technology Limited, Exploring the Science.

Decker, C. (2002). Kinetic study and new applications of UV radiation curing. *Macromolecular Rapid Communications* 23(18): 1067-1093.

Decker, C. (2003). Dualcuring of waterborne urethaneacrylate coatings by UV and thermal processing. *Macromolecular Materials and Engineering* 288: 17-28.

Decker, C., T. V. Nguyen, E. Decker and Weber-Koehl (2001). UV-radiation curing of Acrylate/Epoxide systems. *Polymer* 42: 5531-5541.

Dietliker, L. (1991). *Chemistry & technology of UV & EB formulation for coatings. inks & paints* 3.

Eliades, T., G. Eliades, W. A. Brantley and W. M. Johnston (1995). Residual monomer leaching from chemically cured and visible light-cured orthodontic adhesives. *American Journal of Orthodontics and Dentofacial Orthopedics* 108(3): 316-321.

Hill, L. W. (1997). Calculation of crosslink density in short chain networks. *Progress in Organic Coatings* 31(3): 235-243.

Hillewaere, X. K. D., R. F. A. Teixeira, L.-T. T. Nguyen, J. A. Ramos, H. Rahier and F. E. Du Prez (2014). Autonomous self-healing of epoxy thermosets with thiol-isocyanate chemistry. *Advanced Functional Materials* 24(35): 5575-5583.

Hwang, J. W., K. N. Kim, G. S. Lee, J. H. Nam, S. M. Noh and H. W. Jung (2013). Rheology and curing characteristics of dual-curable automotive clearcoats using thermal radical initiator derived from O-imino-isourea and photo-initiator. *Progress in Organic Coatings* 76(11): 1666-1673.

Jang, E. S. (2012). Recent development in silicone liquid optically clear adhesive (LOCA) for high and large vehicle display touch screen

applications. the Society for Information Display.

Kardar, P., M. Ebrahimi, S. Bastani and M. Jalili (2009). Using mixture experimental design to study the effect of multifunctional acrylate monomers on UV cured epoxy acrylate resins. *Progress in Organic Coatings* 64(1): 74-80.

Kim, M. J., K. H. Kim, Y. K. Kim and T. Y. Kwon (2013). Degree of conversion of two dual-cured resin cements light-irradiated through zirconia ceramic disks. *Journal of Advanced Prosthodontics* 5(4): 464-470.

Kim, S., S.-W. Lee, D.-H. Lim, J.-W. Park, C.-H. Park and H.-J. Kim (2013). Fabrication of optically clear acrylic pressure-sensitive adhesive by photo-polymerization: UV-curing behavior, adhesion performance, and optical properties. *Journal of Adhesion Science and Technology* 27(20): 2177-2190.

Lee, B. C. and D. W. Kang (2007). Preparation and characteristics of silicone modified polyacrylic hybrid elastomer. *Polymer-Korea* 31(1): 86-91.

Lee, S.-W., J.-W. Park, Y.-E. Kwon, S. Kim, H.-J. Kim, E.-A. Kim, H.-S. Woo and J. Swiderska (2012). Optical properties and UV-curing behaviors of optically clear semi-interpenetrated structured acrylic pressure sensitive adhesives. *International Journal of Adhesion and Adhesives* 38: 5-10.

Lovell, L. G., K. A. Berchtold, J. E. Elliott, H. Lu and C. N. Bowman (2001). Understanding the kinetics and network formation of dimethacrylate dental resins. *Polymers for Advanced Technologies* 12(6): 335-345.

Moussa, K. and C. Decker (1993). Light-induced polymerization of new highly reactive acrylic monomers. *Journal of Polymer Science Part A: Polymer Chemistry* 31(9): 2197-2203.

Nelson, E. W., J. L. Jacobs, A. B. Scranton and K. S. Anseth (1995). Photo-differential scanning calorimetry studies of cationic polymerizations of divinyl ethers. *Polymer* 36(24): 4651-4656.

Noh, S. M., J. W. Lee, J. H. Nam, K. H. Byun, J. M. Park and H. W. Jung (2012). Dual-curing behavior and scratch characteristics of hydroxyl functionalized urethane methacrylate oligomer for automotive clearcoats. *Progress in Organic Coatings* 74(1): 257-269.

Park, S., J. W. Hwang, K. N. Kim, G. S. Lee, J. H. Nam, S. M. Noh and H. W. Jung (2014). Rheology and curing characteristics of dual-curable clearcoats with hydroxyl functionalized urethane methacrylate oligomer: Effect of blocked isocyanate thermal crosslinkers. *Korea-Australia Rheology Journal* 26(2): 159-167.

Park, Y.J., D.H. Lim, H.J. Kim, D.-S. Park and I.K. Sung (2009). UV- and thermal-curing behaviors of dual-curable adhesives based on epoxy acrylate oligomers. *International Journal of Adhesion and Adhesives* 29(7): 710-717.

Saiki, N., S. Kainou, H. Shizuhata, H. Seno and K. Ebe (2010). Ultraviolet/heat dual-curable film adhesives with pendant-acryloyl-functional-group-modified epoxy resin. *Journal of Applied Polymer Science*: n/a-n/a.

Satas, D. (1999). *Handbook of pressure sensitive adhesive technology*. New York, Satas & Associates.

Scherzer, T. and U. Decker (1999). Kinetic investigations on the UV-induced photopolymerization of a diacrylate by time-resolved FTIR spectroscopy: the influence of photoinitiator concentration, light intensity and temperature. *Radiation Physics and Chemistry* 55(5-6): 615-619.

Scherzer, T. and U. Decker (1999). Real-time FTIR–ATR spectroscopy to study the kinetics of ultrafast photopolymerization reactions induced by monochromatic UV light. *Vibrational spectroscopy* 19(2): 385-398.

Schmid, U. (2001). Rad Tech Europe.

Shang, Q., S. Hao, J. Zhang, J. Gong, F. Wang, Y. Wu and S. Gu (2015). Investigation on constitution of electrical conductive adhesives fitting for UV–thermal dual curing. *Journal of Adhesion Science and Technology* 29(9): 910-923.

Simić, S., B. Dunjić, S. Tasić, B. Božić, D. Jovanović and I. Popović (2008). Synthesis and characterization of interpenetrating polymer networks with hyperbranched polymers through thermal-UV dual curing. *Progress in Organic Coatings* 63(1): 43-48.

Studer, K., C. Decker, E. Beck and R. Schwalm (2003). Overcoming oxygen inhibition in UV-curing of acrylate coatings by carbon dioxide inerting, Part I. *Progress in Organic Coatings* 48(1): 92-100.

Studer, K., C. Decker, E. Beck and R. Schwalm (2005). Thermal and photochemical curing of isocyanate and acrylate functionalized oligomers. *European Polymer Journal* 41(1): 157-167.

Studer, K., P. T. Nguyen, C. Decker, E. Beck and R. Schwalm (2005). Redox and photoinitiated crosslinking polymerization. *Progress in Organic Coatings* 54(3): 230-239.

Su, Y.-C., L.-P. Cheng, K.-C. Cheng and T.-M. Don (2012). Synthesis and characterization of UV- and thermo-curable difunctional epoxyacrylates.

Materials Chemistry and Physics 132(2-3): 540-549.

Trovati, G., E. A. Sanches, S. C. Neto, Y. P. Mascarenhas and G. O. Chierice (2010). Characterization of polyurethane resins by FTIR, TGA, and XRD. *Journal of Applied Polymer Science* 115(1): 263-268.

Witzel, M. F., F. C. Calheiros, F. Goncalves, Y. Kawano and R. R. Braga (2005). Influence of photoactivation method on conversion, mechanical properties, degradation in ethanol and contraction stress of resin-based materials. *Journal of Dentistry* 33(9): 773-779.

Xia, W. Z. and W. D. Cook (2003). Exotherm control in the thermal polymerization of nona-ethylene glycol dimethacrylate (NEGDM) using a dual radical initiator system. *Polymer* 44(1): 79-88.

Xu, H., F. Qiu, Y. Wang, W. Wu, D. Yang and Q. Guo (2012). UV-curable waterborne polyurethane-acrylate: preparation, characterization and properties. *Progress in Organic Coatings* 73(1): 47-53.

Zhu, S., Y. Tian, A. E. Hamielec and D. R. Eaton (1990). Radical trapping and termination in free-radical polymerization of MMA. *Macromolecules* 23(4): 1144-1150.

초록

현재 디스플레이 접합 공정에는 측면 경화를 포함한 UV 경화 공정이 사용되고 있다. 그러나 UV 경화 공정은 빛이 통하지 않는 음영부를 경화시키지 못하는 치명적인 단점이 있어 디스플레이 접합 공정에서 빛이 통과하지 못하는 베젤 하부에 있는 접착제의 경화가 진행되지 않는 문제가 발생하였다. 하지만 UV 경화는 빠른 경화속도, 무용제형 공정, 저에너지 공정 등의 다양한 장점이 있기 때문에, UV 경화 공정에서의 미경화 문제를 해결하고 그 적용 범위를 향상시키기 위하여 이중경화 방식을 도입하였다.

본 연구에서는 디스플레이 접착용 광학용 투명 접착 소재의 경화를 위하여 고반응성 열개시제를 이용한 이중경화형 접착제의 경화 거동을 분석하고 물성의 평가를 수행하였다. 이를 위하여 30° C 의 10 시간 반감기 온도를 가지는 열 라디칼 개시제인 2,2'-azobis (4-methoxy-2,4-dimethyl valeronitrile)을 이용하여 저온에서의 열 경화 능력을 부여하였다. 디스플레이의 터치 스크린 패널은 100° C 이상의 온도에서 손상을 받을 수 있기 때문에 80° C 에서 열경화를 평가하였다. 사용된 열개시제는 높은 반응성으로 인해 과량 첨가할 경우 황변, 기포, 미용해 등의 문제를 발생시키기 때문에 0.1phr 투입량 이하에서 평가하였다. 또한 공정 중 플렉시블 배선회로기판(FPCB) 및 블랙 매트릭스(BM) 부의 영향으로 인하여 다양한 UV 조사량(0, 400, 800, 1600 mJ/cm²) 조건 하에서 이중경화형 접착제를 제조하였다. 프리폴리머는 UV 별크 중합 방식으로 2-ethylhexyl acrylate, isobornyl acrylate, N-vinyl caprolactam 을 이용하여 합성하였다. 이중경화형

접착제는 프리폴리머, 다기능 단량체, 열 라디칼 개시제를 배합하여 제조하였다.

이중경화형 접착제의 경화 거동을 열적, 점탄성적, 화학적 변화의 다각적 측면에서 평가하였다. 그 결과 열 개시제 함량이 증가함에 따라 열 경화 효율이 증가하였으며, 안정적인 개시제 함량인 0.1phr 에서 충분한 전환율을 확보할 수 있었다. 또한 UV 조사량이 증가함에 따라 고분자의 이동성이 감소하여 열 경화 효율이 점차 감소하지만 낮은 UV 조사량에서는 열 개시 효율이 상승하였다. 겔 분율 분석 결과 이중경화형 접착제의 가교 구조는 800 mJ/cm^2 이상에서 형성되지 못하였으나, 열 경화를 통하여 추가적인 가교구조를 형성할 수 있었다. 열 경화 거동이 촉진됨에 따라 전환율 및 가교도를 확보할 수 있었지만, 경화 거동이 억제되는 800 mJ/cm^2 에서는 400 mJ/cm^2 보다 낮은 전환율과 가교도를 나타내었다. 또한 열 개시제의 반응에 의해 시차주사 열량측정법을 통한 유리전이온도 및 열 저항성이 상승하였다. 이는 UV 경화를 통하여 완전경화 된 이후에도 잔여 단량체와 열 개시제의 반응을 통하여 임시적 물리 가교 구조의 형성이 생성되었기 때문이라고 추측되었다.

UV-ARES 를 이용하여 UV 경화거동, 열 경화거동, 점탄성 특성을 연속적으로 분석하였다. 개시제의 첨가는 UV 경화 시 저장탄성률에 영향을 끼치지 않았다. 이후 열 경화거동은 UV 조사량이 감소함에 따라 향상되었으며 75%의 전환율을 가지게 되는 800 mJ/cm^2 이후에서는 저장탄성률에 영향을 끼치지 못하였다. 고무상 평탄 영역을 이용하여 분석한 결과 낮은 UV 조사 조건에서 이중경화를 진행할 경우 생성된 가교 구조는 더욱 높은 가교밀도를 가지는 것을 확인할 수 있었다. 이에 따라 낮은 열 개시제 함량과 반응 온도에서도 우수한 접착 강도를 확보할 수

있었다. 또한 접착 강도 분석 및 가교도 형성에 대한 결과를 바탕으로 이중경화에 따른 접착제의 분자 구조 형성에 대하여 제시하였다.

주요어: 접착제, UV 경화, 광경화, 접착 강도, 점탄성적 특성,
이중경화형 접착제, 경화 거동, 광학용투명접착제

학번: 2013-23251